

**ATP-conductive channel and ATP release:
Regulation by arachidonic acid and
activation in ischemic conditions**

Amal Kumar Dutta

Department of Physiological Sciences
School of Life Science

The Graduate University for Advanced Studies

ABBREVIATION LIST

CFTR-Cystic fibrosis transmembrane conductance regulator

CoA-Coenzyme A

DMEM-Dulbecco's modified Eagle's medium

DMSO-Dimethyl Sulfoxide

Gd³⁺-Gadolinium

HBSS-Hank's buffer salt solution

MDR-Multidrug-resistance protein

NDGA-Nordihydroguaiaretic acid

NPPB-5-Nitro-2-(phenylpropylamino)-benzoate

PKCε-Protein kinase C epsilon

PLA2-Phospholipase A2

VDACL-Volume-dependent ATP-conductive large-conductance

VSOR-Volume-sensitive outwardly rectifying

SUMMARY

Mouse mammary C127 cells responded to hypotonic stimulation with activation of the volume-dependent ATP-conductive large-conductance (VDACL) anion channel and massive release of ATP. Arachidonic acid down-regulated both VDACL currents and swelling-induced ATP release in physiological concentration range with K_d of 4 – 6 μM . The former effect observed in the whole-cell or excised patch mode was more prominent than the latter effect observed in intact cells. The arachidonate effects were direct and not mediated by downstream metabolic products, as evidenced by their insensitivity to inhibitors of arachidonate-metabolizing oxygenases, and that they were mimicked by *cis*-unsaturated fatty acids, which are not substrates for oxygenases. A membrane-impermeable analog arachidonyl coenzyme A was effective only from the cytosolic side of membrane patches suggesting that the binding site is localized intracellularly. Non-charged arachidonate analogs as well as *trans*-unsaturated and saturated fatty acids had no effect on VDACL currents and ATP release, indicating the importance of arachidonate's negative charge and specific hydrocarbon chain conformation in the inhibitory effect. VDACL anion channels were inhibited by arachidonic acid in two different ways: channel shutdown (K_d of 4 – 5 μM) and reduced unitary conductance (K_d of 13 – 14 μM) without affecting voltage dependence of open probability. ATP^{4-} -conducting inward currents measured in the presence of 100 mM ATP in the bath were reversibly inhibited by arachidonic acid. Thus, I conclude that swelling-induced ATP release and its putative pathway, VDACL anion channel, are under a negative control by intracellular arachidonic acid signaling in mammary C127 cells.

In primary culture of neonatal rat cardiomyocytes, hypotonic and ischemic conditions induced ATP release. The release of ATP both in ischemic and hypotonic conditions were time-dependent detected by luciferine/luciferase ATP assay method. The local concentration of ATP during hypotonic and ischemic conditions exceeded micromolar levels detected by biosensor technique. The same stimulus activated Volume-dependent ATP-conductive Large-conductance Anion (VDACL) channel in neonatal rat cardiomyocytes, in cell-attached configuration of patch clamp. Hypoxia mimicked the results of hypotonic and chemical ischemic conditions. Under isotonic conditions, cell-attached patches were normally silent, but patch excision led to the activation of

currents that consisted of multiple large-conductance unitary steps. The currents displayed voltage- and time-dependent inactivation, similar to C127 cells in our previous study (Sabirov et al. JGP 2001, 118: 251-266). The single-channel conductance was app. 400 pS, with linear current-voltage relationship. The channel was anion selective and exhibited ATP-permeability with $P_{\text{ATP}}/P_{\text{Cl}}$ of ~ 0.1 . In contrast to VDACL (~ 400 pS), cardiomyocytes contained single channel events with unitary conductance of app. half of VDACL size (~ 250 -200 pS). Voltage dependency, anion selectivity and ATP permeability of this channel were similar to VDACL. I suppose that this smaller amplitude represents a sub-state of fully open VDACL channel. These sub-states were predominant in cell-attached patch mode (specially in hypoxic conditions) than in inside-out mode. The VDACL channel activity and swelling-induced ATP release were inhibited by NPPB, SITS, Gd^{3+} , and arachidonic acid, but was insensitive to glibenclamide. Thus it is concluded that pathophysiological conditions like, cell-swelling and ischemia induced ATP release, and cardiac VDACL channel could serve as a conductive pathway for ATP release.

INTRODUCTION

ATP is not only an energy source but also acts as an auto- and para-crine regulator of numerous cellular functions (Bodin & Burnstock, 2001). Every cell contains milimolar levels of ATP but interstitial level of ATP is around nanomolar level (Vassort, 2001). Local concentration of ATP can exceed micromolar level due to regulated release. In some pathophysiological situations local concentration of ATP exceed 100 μ M temporarily (Coade & Pearson, 1989). ATP could be released due to cell injury by wounding, necrosis, inflammation, degranulation and so on. Neurons, mast cell and glandular cells release ATP by exocytosis. At the same time non-exocytotic ATP release may occur from endothelial, epithelial, muscle and other cells. ATP released from cardiac tissue upon various stimuli specially hypoxia (Vial *et al.* 1987; Borst and Schrader, 1991; Forrester and Williams, 1977), ischemia/reperfusion (Kuzmin *et al.* 2000,1998; Vassort, 2001; Ninomiya *et al.* 2001). Mechanical stress and osmotic swelling are among the most effective physiological stimuli for ATP release (Burnstock, 1999; Bodin & Burnstock, 2001). Cell swelling is known to induce ATP release from various cells type (Wang *et al.* 1996; Roman *et al.* 1997, 1999; Feranchak *et al.* 1998; Hazama *et al.* 1998b, 1999, 2000a,b; Mitchell *et al.* 1998; Taylor *et al.* 1998; Light *et al.* 1999; Musante *et al.* 1999; Sabirov *et al.* 2001). Released ATP can either be degraded by ecto-ATPases to ADP, AMP and adenosine, or it can bind to P2 receptors and trigger a variety of cellular responses (Guy Vassort, 2001). Extracellular ATP may cause arrhythmia, vasoconstriction and vasodilatation, smooth muscle tone modulation of GIT and urinary bladder. It may be involved in fluid secretion in airway and intestinal epithelia, platelet aggregation, nociception and many other functions.

Although purinergic receptor proteins located on the plasma membrane are well characterized, the molecular nature of the ATP-releasing pathway remains poorly understood at present. As most ATP molecules exist in anionic forms at physiological pH, it is plausible that some anion channels can conduct ATP, thereby serving as a pathway for ATP release. Indeed, ATP-conducting currents associated with the expression of CFTR or MDR1 (Reisin *et al.* 1994; Schwiebert *et al.* 1995; Cantiello *et al.* 1997, 1998; Pasyk and Foskett, 1997; Lader *et al.* 2000) or MDR1 (Abraham *et al.* 1993; Bosch *et al.* 1996; Roman *et al.* 1999), or independent of CFTR and MDR1 expression (Grygorczyk & Hanrahan, 1997; Sugita *et al.* 1998; Bodas *et al.* 2000) have so far been observed. We recently demonstrated that in mouse mammary C127 cells

(Hazama *et al.* 2000b) and human Intestine 407 cells (Hazama *et al.* 1999) neither CFTR nor volume-sensitive outwardly rectifying (VSOR) Cl^- channels were responsible for swelling-induced release of ATP. On the other hand, we demonstrated (Sabirov *et al.* 2001) that cell swelling activated not only conventional VSOR channels but also another type of anion channel which exhibits a large unitary conductance (~ 400 pS), bell-shaped voltage dependence and ATP permeability. This Volume- (and voltage-) **D**ependent **A**TP-**C**onductive **L**arge conductance (VDACL) anion channel had a pharmacological profile distinct from that of the VSOR channel, but strikingly similar to that of swelling-induced ATP release, and thus the VDACL channel was proposed to be an ATP-releasing conductive pathway in mammary C127 cells (Sabirov *et al.* 2001).

At present, little information is available on physiologic regulators of swelling-induced ATP release machinery in general and the VDACL channel as a putative pathway of ATP release in particular. Arachidonic acid is an unsaturated fatty acid liberated from membrane phospholipids by phospholipases (Irvine, 1982; Holtzman, 1991; Meves, 1994; Brash, 2001) upon stimulation by a variety of stimuli, including hypotonic stress (Thoroed *et al.* 1997; Tinel *et al.* 1997; Basavappa *et al.* 1998; Pedersen *et al.* 2000; Hoffmann, 2000). Thus, I tested the hypothesis that the arachidonic acid signaling pathway is involved in the regulation of swelling-induced ATP release mediated by the VDACL channel. Here I report that arachidonic acid, at physiologically relevant concentrations, downregulates both VDACL channel activity and swelling-induced ATP release in C127 cells, a fact providing new evidence that the VDACL channel serves a pathway for swelling-induced ATP release in C127 cells. Also, I provide evidence that anionic arachidonate exerts a downregulatory effect from the intracellular side of the VDACL anion channel, not only by reducing the number of active channels but also by reducing the unitary conductance of open channels. A negative charge and the *cis*-conformation of hydrophobic chain constitute the structural determinants essential for the inhibitory activity of arachidonic acid.

In the mammalian heart ATP and hydrolytic metabolites, chief among which are adenosine, exert profound electrophysiological effects including a negative chronotropic effect on cardiac pacemakers and dromotropic effects on atrial-ventricular node (Pelleg *et al.*, 1990). On a single cardiomyocytes, micromolar ATP induces nonspecific cationic and chloride currents that depolarize the cells. P_2 -purinergic

stimulation increases cAMP by activating adenylyl cyclase (Vassort, 2001). Extracellular ATP has been shown to regulate Na⁺ (Scamps and Vassort, 1994), muscarinic acetylcholine K⁺ (Shoda et al., 1997), L-type Ca²⁺ channel (Qu *et al.*, 1993) and different types of chloride channels function (Vassort, 2001; Levesque & Hume 1995). Extracellular ATP known to regulate cell volume by activating volume sensitive Cl⁻ channels (Wang *et al.* 1996).

The source of ATP in extra-cellular space during hypoxia, ischemia/reperfusion in cardiac tissue could be various; (Burnstock, 1972; Forrester and Williams, 1977). The released ATP may cause vasoconstriction via P2X- and vasodilatation via P2Y-purinoreceptors of coronary vessels (Hopwood and Burnstock, 1987). In ischemic preconditioning ATP may play an essential role by itself or/and by its degradation product adenosine (Ninomiya *et al.* 2001; Vassort, 2001; Cohen *et al.* 2000; Kuzmin *et al.* 2000). Although purinergic receptor proteins located on the sarcolemma are characterized (Burnstock and Kennedy, 1986), the source of ATP and the molecular nature of the ATP-releasing pathway poorly known during cell swelling, hypoxia and ischemia/reperfusion.

I extended my study to detect ATP release as well as VDACL channel expression in primary culture of neonatal rat cardiomyocytes. I developed a new superfusion system to measure time dependency of ATP release, by luciferin/luciferase ATP assay method, in hypotonic, ischemic as well as hypoxic conditions. The local concentration of ATP can exceed micromolar levels (detected by PC12 biosensor method), necessary to activate P₂ receptors, present on the sarcolemma (Vassort, 2001). VDACL, demonstrated as a conductive pathway for ATP release in C127 cells (Sabirov *et al.* 2001), also activated in primary culture of neonatal rat cardiomyocytes, in hypotonic, ischemic as well as hypoxic conditions. The biophysical and pharmacological properties of cardiac VDACL are similar to VDACL in C127 cells, in our previous study (Sabirov *et al.* 2001).

MATERIALS AND METHODS

Cells

A cell line of mouse mammary tissue origin, C127, was obtained from the American Type Culture Collection and grown in Dulbecco's modified Eagle's medium containing 10% FCS. For single-channel patch-clamp experiments, the cells were grown on glass coverslips. For whole-cell recordings, the cells attached on the plastic substrate were resuspended by mechanical detachment, as reported previously (Kubo and Okada, 1992), and cultured with agitation for 15-300 min. Then cells were placed in a chamber and washed by bathing solution after attaching them to the glass bottom of the chamber. For ATP assays, C127 cells were cultured to confluence in 24-well plates.

Neonatal rat cardiomyocytes were prepared using a method, described elsewhere (Simpson and Savion, 1982) with some modification. Briefly, 2-3 days old Wistar rat hearts were excised; blood, connective tissue and atria were removed carefully, and ventricles were cut into ~2 mm pieces and placed into 4 ml of 0.05% Trypsin solution in HBSS (GIBCO BRL, Life Technologies, New York, USA) containing 0.53 mM EDTA. The tissue was subjected to 4-5 successive 15 min periods of dissociation with gentle stirring in 5%-CO₂ incubator. The first supernatant was discarded; each of the following supernatants were collected and moved into 20 ml of M199 culture medium (Nissui, Tokyo, Japan) supplemented with 20% of newborn bovine serum. M199 culture medium with supernatants were pooled and centrifuged at 600 rpm for 5 min. Cells were resuspended in M199 medium supplemented with 10% of newborn bovine serum, centrifuged once at 600 rpm for 3 min, resuspended in the same medium and placed in 35-mm culture dishes for one hour. Non-adherent cells (cardiac myocytes) were plated on glass cover slips for patch-clamp experiments and ATP release measurement.

PC12 cells were obtained from Riken Cell Bank (Tsukuba, Japan), cultured in DMEM supplemented with 10% fetal bovine serum, and used for patch-clamp experiments without inducing differentiation.

Solutions

The standard Ringer solution contained (mM): 135 NaCl, 5 KCl, 2 CaCl₂, 1 MgCl₂, 5 Na-HEPES, 6 HEPES, 5 glucose (pH 7.4, 290 mosmol kg⁻¹ H₂O). The hypotonic

solution for whole-cell recording was made by reducing the concentration of NaCl in Ringer solution to 100 mM (210 mosmol kg⁻¹ H₂O). Isotonic bath solution for whole-cell experiments was made from this hypotonic solution by adding 80 mM mannitol. The bath (intracellular) solution for inside-out experiments contained (mM): 130 KCl, 10 NaCl, 1 MgCl₂, 6 HEPES, 5 Na-HEPES, 4.16 CaCl₂, 5 EGTA (pH 7.4 adjusted with KOH, osmolality 302 mosmol kg⁻¹ H₂O). In the inside-out experiments for C127 cells pCa was buffered at 6.3, although Ca²⁺ in a range from 15 nM up to 2 mM had no significant effect on VDACL channel behavior and its inhibition by arachidonic acid (data not shown). The pipette (intracellular) solution for whole-cell and outside-out (in case of cardiomyocytes) experiments contained (mM): 125 CsCl, 2 CaCl₂, 1 MgCl₂, 5 HEPES, 10 EGTA (pH 7.4 adjusted with CsOH, pCa 7.6, osmolality 275 mosmol kg⁻¹ H₂O). The pipette (extracellular) solution for inside-out experiments was standard Ringer solution. The pipette (intracellular) solution for outside-out experiments contained (mM): 120 NaCl, 5 KCl, 2 CaCl₂, 1 MgCl₂, 5 HEPES, 10 EGTA (pH 7.4 adjusted with NaOH, pCa 7.5, osmolality 275 mosmol kg⁻¹ H₂O). ATP was omitted from intracellular solutions (pipette solutions for whole-cell and outside-out and bath solution for inside-out experiments) in order to avoid the activation of VSOR Cl⁻ currents in whole-cell measurements and to minimize the modulatory effect of ATP on VDACL channel in excised patches (Sabirov *et al.* 2001). In cardiomyocytes experiments, in on-cell mode, Ca²⁺ free solution was used. For selectivity measurement, instead of NaCl and KCl, 140 NMDGCl or 135 Na-glutamate were used in Ringer solution. In some experiments, all monovalent cations were replaced by TEA-Cl, in pipette solution. For ATP-mediated current measurements, 100 mM Na₂ATP solution was used after pH was adjusted at 7.4 with NaOH. All ATP-containing solutions were kept on ice and warmed to room temperature immediately before the experiment.

For chemical ischemic conditions, instead of 5 mM glucose, 10 mM 2-deoxy-D-glucose (2DG) and 5 mM NaCN were added in control solution (pH was adjusted to 7.4). For hypoxic conditions, 100% argon gas was used for continuous bubbling one hour before starting experiment as well as during experiment.

The osmolality of all solutions were measured using a freezing-point depression osmometer (OM802, Vogel, Germany).

Chemicals

Fatty acids were added to their final concentrations just before the experiments from stock solutions (40 mM or 200 mM in DMSO). Indomethacin, nordihydroguaiaretic acid (NDGA) and clotrimazole (all from Sigma-Aldrich) were added from stock solution of 20 mM in DMSO to their final concentrations just before the experiments. 5-Nitro-2-(phenylpropylamino)-benzoate (NPPB), glibenclamide, 4-acetamino-4'-isothiocyanostilbene (SITS), Suramin (all from Sigma-Aldrich) were added to Ringer's solution immediately before use from stock solutions in DMSO to the final concentrations as indicated. The final DMSO concentration did not exceed 0.1% and DMSO did not have any effects, when added alone. Apyrase, deoxyglucose (from WAKO) added to bath solution when needed. GdCl_3 was stored as a 50-mM stock solution in water and added directly to Ringer's solution immediately before the experiment.

Electrophysiology

Patch electrodes were fabricated from borosilicate glass using a micropipette puller (P-97, Sutter Instrument, Novato, CA) and had a tip resistance of about 2 M Ω for whole-cell current measurements and 2-5 M Ω for macro-patch and single-channel recording when filled with pipette solutions. For whole-cell recordings, access resistance did not exceed 5 M Ω and was always compensated (to 70 – 80%). Membrane currents were measured with an Axopatch 200A patch-clamp amplifier coupled to a DigiData 1200 or DigiData 1322A interface (Axon Instruments, Union City, CA, USA). Unless otherwise specified, currents were filtered at 1 kHz and sampled at 1 – 5 kHz. Data acquisition and analysis were done using pCLAMP 6 and 8.1 (Axon Instruments) and WinASCD software (provided by Dr. G. Droogmans, KU Leuven, Belgium). Whenever bath chloride concentration was changed, a salt bridge containing 3M KCl in 2% agarose was used to minimize bath electrode potential variations. Liquid junction potentials were calculated using pCLAMP 8.1 algorithms and corrected when necessary. All experiments were performed at room temperature (20-22°C).

Luciferin-Luciferase ATP Assay

Bulk extracellular ATP concentration was measured by the luciferin-luciferase assay (ATP Luminescence Kit; AF-2L1, DKK-TOA Co., Tokyo, Japan) at 37°C as described previously (Hazama *et al.* 1999, 2000b; Sabirov *et al.* 2001), with slight modifications. Briefly, C127 cells were cultured to confluence in 24-well plates. Culture medium was totally replaced with 425 µl of normal Ringer solution. Cells were incubated for 60 min at 37°C, and 100 µl of isotonic extracellular solution was removed and used as a control sample for background ATP release measurements. A hypotonic challenge was then applied by gently removing 300 µl of supernatant and adding 400 µl of a solution of desired tonicity. Hypotonic solutions were made by mixing Ringer solution with an appropriate volume of a solution of the following composition (mM): 5 KCl, 2 CaCl₂, 1 MgCl₂, 5 Na-HEPES, 6 HEPES, 5 glucose (pH 7.4, 40 mosmol kg⁻¹ H₂O). The cells were then incubated for 15 min at 37°C, and extracellular solution samples (100 µl) were collected for the luminometric ATP assay of swelling-induced ATP release. ATP concentration was measured by mixing 50 µl of sample solution with 500 µl normal Ringer solution and 50 µl of luciferin-luciferase reagent. At this ratio, ionic salt sensitivity of luciferase reaction (Boudreault & Grygorczyk, 2002) was negligible. When required, arachidonic acid, fatty acids and metabolic inhibitors were added during the 60 min preincubation and 15 min hypotonic stimulation periods. Arachidonic acid and other fatty acids tested had no appreciable effect on luciferin-luciferase reaction.

In case of ATP measurement from cultured neonatal rat cardiomyocytes, round 12-mm cover glass with cultured neonatal rat cardiomyocytes, were superfused by control solution in a perfusion chamber, at a rate of 1.5 ml/min (to minimize the shear stress effect on ATP release), at room temperature. The superfusate was collected every minute for measurement of released ATP concentration. After a steady-state level of ATP in control condition, the solution was replaced by solutions indicated in the Results section. In order to minimize the ionic sensitivity of luciferine/luciferase reaction (Boudreault & Grygorczyk, 2002), the tonicity of solution was changed by adding or removing mannitol (same solutions as used in patch-clamp experiment). An aliquot (500 µl) of perfusate was mixed with 50 µl of luciferin/luciferase assay mixture for luminometric ATP measurement. Since Gd³⁺ was reported to interfere with

luciferase reaction (Boudreault and Grygorczyk 2002), I supplemented the luciferin/luciferase assay mixture with 600 μM of EDTA in experiments with effect of GdCl_3 on ATP release. In this condition, Gd^{3+} (50 μM) still decreased the luminescence by $\sim 20\%$. However, this effect was much weaker compared to its effect on the ATP release. Other inhibitors had no significant effect on luciferin-luciferase reaction.

Detection of ATP release by Biosensor technique

The method was originally established by Hazama et al. (1998) and described elsewhere. Briefly, conventional whole-cell recordings from PC12 cells were made in bath chamber, with or without cardiomyocytes, at a holding potential of -50 mV . During recording with cardiomyocytes, voltage-clamped PC12 cells were placed very close to the center of cardiomyocytes. When needed, bath solution was changed to the hypotonic or ischemic solutions as indicated. In calibration experiments, ATP was applied to a PC12 cell without attaching to a cardiomyocytes, through a micropipette filled with ATP-containing bath solution.

Data analysis

Single-channel amplitudes were measured by manually placing cursors at the open and closed channel levels. Mean patch currents were measured at the beginning (first 25 – 30 ms) of current traces in order to minimize the contribution of voltage-dependent current inactivation.

Concentration-response data for arachidonic acid inhibition of macro-patch currents and single-channel currents were fitted to the following equation:

$$I/I_o = 1/(1 + (X/K_d)^h), \quad (1)$$

Where I_o is the current in the absence of arachidonic acid, I is the current in the presence of arachidonic acid at the concentration $[X]$, K_d is the apparent dissociation constant, and h is the Hill coefficient.

Dose-response data for arachidonic acid inhibition of swelling-induced ATP release were fitted to the following equation:

$$A = (A_0 - A_1)/(1 + (X/K_d)^h) + A_1, \quad (2)$$

Where A_o is the released ATP level in the absence of arachidonic acid, A is that in the presence of arachidonic acid at the concentration $[X]$, A_I is the non-inhibited fraction of released ATP, K_d is the apparent dissociation constant, and h is the Hill coefficient.

Permeability ratios for different anions (X) were calculated from Goldman-Hodgkin-Katz (GHK) equation:

$$\Delta E_{rev} = -RT/F \ln [(P_{Cl}[Cl]_o)/(P_{Cl}[Cl]_i + P_X[X])], \quad (3)$$

where ΔE_{rev} is the reversal potential in presence of a test anion at a concentration $[X]$, $[Cl]_o$ is the Cl^- concentration in the pipette (standard Ringer solution), and $[Cl]_i$ is the Cl^- concentration in low Cl^- bath solutions containing different test anions. P_{Cl} and P_X are the permeabilities of Cl^- and test anion, respectively.

Permeability ratio for ATP were calculated from Goldman-Hodgkin-Katz (GHK) equation:

$$P_A/P_{Cl} = \{z_{Cl}^2 [[Cl]_o - [Cl]_i \exp(\alpha z_{Cl} E_{rev})][1 - \exp(\alpha z_A E_{rev})]\} / \{z_A^2 [A]_i \exp(\alpha z_A E_{rev})[1 - \exp(\alpha z_{Cl} E_{rev})]\}, \quad (4)$$

where $\alpha = F/RT$; z_A and z_{Cl} are valences of ATP and Cl^- , respectively; $[Cl]_o$ and $[Cl]_i$ are the Cl^- concentrations in the pipette and in the bath, respectively; $[A]_i$ is the ATP concentration in the bath; and E_{rev} is the reversal potential. When no Cl^- was present in the bath, and therefore $[Cl]_i = 0$, the equation turns to the one used in Cantiello et al. (1997). z_A was assumed to be -4 for ATP.

Data were analyzed in Origin 5.0 (OriginLab Corp., Northampton, MA, USA). Pooled data are given as means \pm SEM of observations (n). Statistical differences of the data were evaluated by paired or unpaired Student's t test and considered significant at $P < 0.05$ (or $P < 0.01$ when indicated).

In all figures, membrane potential (V_m) is indicated according to the convention: $V_m = V_p$ (the pipette potential) for whole-cell and outside-out experiments, and $V_m = -V_p$ for on-cell and inside-out experiments.

RESULTS

Regulation of the ATP-Conductive Large-Conductance Anion (VDACL) channel and swelling-induced ATP release by arachidonic acid in C127 cells

Arachidonic acid sensitivity of whole-cell VDACL anion currents

In our previous study, we demonstrated that C127 cells express the VDACL anion channel, which shares the same pharmacology with swelling-induced ATP release measured at 25 or 37°C (Sabirov *et al.* 2001). In the whole-cell recording mode, VDACL currents could selectively be recorded when conventional volume-sensitive outwardly rectifying (VSOR) chloride currents were suppressed by omitting ATP from the pipette solution and by supplementing the hypotonic bath solution with phloretin, a relatively selective blocker of VSOR Cl^- channels (Fan *et al.* 2001). Figure 1 A shows the activation of hypotonicity-induced phloretin-insensitive whole-cell VDACL anion currents which exhibited characteristic voltage-dependent inactivation at both positive and negative potentials greater than ± 20 mV (Fig. 1 Ba). The reversal potential of about +5 mV was close to the Nernst potential for Cl^- (+4.2 mV). Bath application of 20 μM arachidonic acid significantly reduced the whole-cell VDACL current (Fig. 1 A and Bb). Arachidonic acid effectively inhibited both inward and outward currents in a voltage-independent manner (Fig. 1 C). In 3 experiments out of 10 attempts was I able to recover the whole-cell current after washing out arachidonic acid. In 7 other experiments, the whole-cell configuration was lost upon washout, possibly due to destabilizing effect of arachidonate on the giga-ohm contact.

Arachidonic acid sensitivity of macropatch VDACL currents in inside-out and outside-out patches

We reported previously that VDACL channels could be activated in cell-attached patches by cell swelling and also could be observed in excised patches (Sabirov *et al.* 2001). Figure 2A shows the inhibition of mean patch current after application of 20 μM arachidonic acid to the bath in an inside-out membrane patch. The effect of arachidonic

acid was reversible. Arachidonic acid inhibited VDACL currents dose-dependently with K_d of $3.9 \pm 0.21 \mu\text{M}$ and $4.44 \pm 0.23 \mu\text{M}$ for outward and inward currents measured at +25 mV and -25 mV, respectively (Fig. 2 Aa).

Similar reversible inhibition was observed when arachidonic acid was applied from the extracellular side to an outside-out patch after steady-state activation of VDACL channels (Fig. 2 B). Inhibition of VDACL currents by external arachidonic acid was also dose-dependent with K_d of $4.99 \pm 0.44 \mu\text{M}$ and $4.54 \pm 0.37 \mu\text{M}$ for outward and inward currents measured at +25 mV and -25 mV, respectively (Fig. 2 Bb). The dose-response curves (Figs. 2 Ab and Bb) could be well fitted with a Hill coefficient of 2, but not 1, implying that more than 1 arachidonic acid molecule is needed to inhibit VDACL channels in both inside-out and outside-out patches.

Since fatty acids are known to move rapidly across phospholipid bilayers (Kamp & Hamilton, 1993), inhibition observed in the outside-out mode does not necessarily mean that arachidonic acid exerted the action from the outside of the channel. In order to clarify the sidedness of the effect, I tested a membrane-impermeable analog arachidonyl coenzyme A (Arachidonyl CoA: Smirnov & Aaronson, 1996; Denson *et al.* 2000). Arachidonyl CoA inhibited the macropatch VDACL currents when applied from the intracellular side in inside-out patches (Fig. 3 A) to the same extent as arachidonic acid, whereas coenzyme A by itself at 20 μM had no effect on the VDACL channel ($n=5$, data not shown). In contrast, arachidonyl CoA added from the extracellular side had no effect in the outside-out mode (Fig. 3 B). The averaged data are summarized in Fig. 3 C. This result suggests the arachidonic acid binding site of the VDACL channel is localized intracellularly.

Direct effects of arachidonic acid on VDACL currents without metabolism by oxygenases

Arachidonic acid, after liberation from membrane phospholipids, is metabolized into different biologically active compounds such as prostaglandins by the cyclooxygenase pathway, leukotrienes by the lipoxygenase pathway, and epoxides by the monooxygenase pathway (Holtzman, 1991). Therefore, in order to distinguish between a direct effect of arachidonic acid on VDACL channel and an indirect inhibition via

metabolic products of one of these oxygenases, which might have been retained on or near the excised patches, we used relatively selective blockers of these pathways: indomethacin, an inhibitor of cyclooxygenase; NDGA, a lipoxygenase inhibitor; and clotrimazole, a cytochrome P-450 monooxygenase inhibitor (Rainsford, 1988). Figure 4 shows that arachidonic acid effectively inhibited macropatch VDACL currents in the presence of these oxygenase inhibitors, whereas these inhibitors themselves did not cause any effect on VDACL currents in inside-out patches. The steady-state level of arachidonate-induced inhibition in the presence of each inhibitor did not differ significantly from that in the absence of these inhibitors (Fig. 4 D). These results indicate that the arachidonic acid effect on VDACL currents was not mediated by its downstream metabolic products and was due to a direct interaction with the channel (or its accessory) protein.

Next I tested whether other fatty acids, which are not substrates for any oxygenases, are also able to inhibit this channel. Indeed, *cis*-unsaturated fatty acids, such as oleic and linoleic acid, inhibited macropatch VDACL currents albeit to a lesser degree than arachidonic acid (Fig. 5 A, B). In contrast, a *trans*-unsaturated fatty acid, elaidic acid, and a saturated fatty acid, palmitic acid, did not affect noticeably the VDACL currents (Fig. 5 A). Therefore, not only hydrophobicity but also the specific conformation of the hydrocarbon chain are important for the inhibitory effect of arachidonic acid on the VDACL channel. Non-charged analogs of arachidonic acid, arachidonyl alcohol and arachidonyl methyl ester, did not have any inhibitory effect on VDACL channels (Fig. 5 C). In addition, although oleic acid was an effective VDACL inhibitor (Fig. 5 A), its neutral analog, oleyl alcohol, was ineffective (Fig. 5 C). These data suggest that the negatively charged polar head is essential for the inhibitory effect of arachidonic acid. Since arachidonyl CoA does not have a carboxylic group but has phosphate residues constituting of a bulky negatively charged polar head, it is suggested that the negative charge, but not the carboxylic group *per se*, is essential for the inhibitory action of arachidonic acid.

Unitary conductance-reducing effect of arachidonic acid on VDACL channels

Arachidonic acid not only inhibited macropatch currents but also reduced the amplitude of the VDACL channel unitary current. Figure 6 A shows inside-out single-channel records in the absence and presence of 10 μ M arachidonic acid in the bath. Even in the

presence of 10 μM arachidonic acid, the single-channel activity could be observed in a small number of remaining active channels, after the activity of most channels was abolished. The single-channel amplitude of both outward and inward events was diminished by arachidonic acid (Fig. 6 B), while the current-voltage relationship remained linear and symmetrical (Fig. 6 C), suggesting a voltage-independent block. The single-channel conductance obtained from the linear fit to I-V curves (Fig. 6 C) decreased from 405.6 ± 6.4 pS to 249.2 ± 7.2 pS by 10 μM arachidonic acid. The arachidonate-induced inhibition of single-VDACL channel activity was dose-dependent with K_d of 13.8 ± 1.6 μM for outward currents and K_d of 14.0 ± 1.1 μM for inward currents (Fig. 6 D). The Hill coefficient was estimated to be 2, but not 1, by fitting all the single-channel dose-response data, implying that this effect of arachidonic acid was also mediated by more than 1 molecule.

No remarkable increase in open-channel noise could be detected in the presence of 10 μM arachidonic acid at +25 mV even when inside-out single-channel recordings were performed at a 5 kHz bandwidth (Fig. 7). This result suggests that voltage-independent single-channel inhibition by arachidonic acid was induced by reduction of single-channel conductance due to either fast (faster than 5 kHz) open-channel block or a conformational change of the open channel pore. Although slightly flickering events were observed at -25 mV in the presence of arachidonic acid (Fig. 7 A), this did not contribute significantly to the observed inhibition of single-channel amplitude, as the K_d values for single-channel amplitudes were voltage-independent.

Shutdown effect of arachidonic acid on VDACL channels

The inhibitory effect of arachidonic acid on macropatch currents was significantly stronger ($K_d = 4 - 5$ μM) than that on single-channel amplitudes ($K_d = 13 - 14$ μM). Figure 8 A summarizes the inhibitory effect of 10 μM arachidonic acid on macropatch currents in comparison to that on single-channel amplitudes at positive and negative potentials. Both outward and inward currents were suppressed much more prominently in macropatches. Results that were essentially the same were observed when arachidonic acid was applied in the presence of a cocktail containing three different oxygenase inhibitors (indomethacin, NDGA and clotrimazole) (Fig. 9 B). These data

indicate that arachidonic acid reduced not only the single-channel amplitude but also the open-channel probability or the number of active channels.

In order to estimate the effect of arachidonic acid on the open-channel probability of the VDACL channel, we applied a series of slow ramp-pulses and recorded the steady-state current responses from the patches containing several channels. Channels always stayed open at potentials near 0 mV ($P_o = 1$) and closed gradually when the membrane potential exceeded 10 – 20 mV yielding a bell-shaped steady-state voltage dependence of open-channel probability (Fig. 8 C) similar to that observed previously (Sabirov *et al.* 2001). The patch shown in Fig. 8 C contained 6 channels, as judged from the stepwise current inactivation at positive and negative voltages. Application of 5 μ M arachidonic acid (sufficient to cause a 50% reduction in macropatch currents) decreased the number of active channels from 6 to 3, but did not have any effect on the steady-state voltage dependence of open-channel probability (Fig. 8 C, open circles), suggesting that arachidonic acid has a negligible effect on the open-channel probability of the VDACL channel. The same result was obtained in 3 other independent experiments.

Macroscopic current (I) is a product of number of active channels (N), single-channel current amplitude (i) and open-channel probability (P_o):

$$I = N i P_o$$

Given the absence of any effect on P_o , I conclude that arachidonic acid exerts dual effects on the VDACL channel: a strong binding to the channel (or its accessory) protein with K_d of 4 – 5 μ M results in channel shutdown (decrease in N), whereas weaker binding to the channel lumen with K_d of 13 – 14 μ M causes a decrease in single-channel amplitude (i).

Arachidonic acid sensitivity of ATP currents through VDACL channels and of swelling-induced ATP release

In our previous study, we demonstrated that the VDACL channel serves as a conductive pathway for swelling-induced ATP release in C127 cells (Sabirov *et al.* 2001). As a natural extension, I tested whether both ATP currents through VDACL channels and swelling-induced ATP release are similarly sensitive to arachidonic acid. Figure 9 A shows records of ionic current from an inside-out patch after replacing the bath (intracellular) solution with 100 mM Na_4ATP . Small but sizable inward currents

that correspond to electrogenic flux of anionic forms of ATP (mainly ATP^{4-}) from bath to pipette through VDACL channels could be recorded, as reported previously (Sabirov *et al.* 2001). Although voltage-dependent inactivation of the ATP^{4-} current was often detectable at -50 mV (Fig. 9 C, top trace), it was not as profound as that of Cl^- current recorded in normal bath solution, suggesting a possibility that the voltage-dependent inactivation profile may somehow be affected by conducting anionic species. Both outward Cl^- currents and inward ATP^{4-} currents were simultaneously inhibited by 20 μM arachidonic acid. In 9 of 12 similar experiments, I was able to restore ATP channel activity upon washout with arachidonate-free Na_4ATP solution. The current traces recorded in this experiment before (a) and during (b) application of arachidonic acid, and after recovery (c), are shown in Fig. 9 B. Fig. 9 C shows more prolonged records of the ATP^{4-} currents obtained in three other experiments.

Hypotonic cell swelling induced massive release of ATP from C127 monolayers in a dose-dependent manner (Fig. 10 A). Arachidonic acid added at 20 μM concentration significantly inhibited swelling-induced ATP release (Fig. 10 A). The inhibition was dose-dependent with K_d of 6.2 ± 0.3 μM (Fig. 10 B). This value is very close to the K_d value obtained for macropatch VDACL currents (Fig. 2 Ab and Bb). It should be noted, however, that even at the highest concentrations tested, arachidonic acid inhibited the ATP release only partially. When the inhibitor cocktail containing three different oxygenase inhibitors (indomethacin, NDGA and clotrimazole, 20 μM each) was applied, the swelling-induced ATP release was suppressed by about 40% even without addition of arachidonate. The remainder of ATP release could be further inhibited by arachidonic acid in a dose-dependent manner with K_d of 4.4 ± 1.2 μM . This value is close to that obtained in the absence of oxygenase inhibitors. Incomplete inhibition in the absence of oxygenase inhibitors may be largely explained by the fact that the effective arachidonic acid concentration decreases. Also, it is possible that downstream metabolic products may antagonize the direct effect of arachidonic acid on the VDACL channel.

Cis-unsaturated fatty acids, oleic and linoleic acid, inhibited ATP release to the same degree as arachidonic acid (Fig. 10 C). In contrast, a *trans*-unsaturated fatty acid, elaidic acid, and a saturated fatty acid, palmitic acid, did not noticeably affect the swelling-induced ATP release (Fig. 10 C). The effect of each fatty acid on ATP release

was qualitatively similar to the effect of each fatty acid on VDACL channel activity in macropatches (Fig. 5).

ATP release and activation of the VDACL channel by hypotonic and ischemic stimulation of primary culture neonatal rat cardiomyocytes

Hypotonicity and ischemic condition induce ATP release from cardiomyocytes

In this study, I used two different approaches to validate the ATP release from cardiac myocytes: i) superfusing the cells grown on glass coverslips and collecting the perfusate for off-line measurement of the released ATP using conventional luciferin-luciferase assay; ii) the biosensor technique.

In the first approach, I superfused the cells at constant rate for 15 min in order to achieve low basal level of ATP in superfusate. This level was rather variable and ranged from 3 to 57 pM depending on cell density and cell preparation. In order to account for the variability of the basal ATP levels, I normalized all the measured ATP concentrations to the average ATP concentration calculated from five consecutive determinations immediately before switching to hypotonic solution. In 13 experiments included into the Fig. 11A, the mean value for these averages was 22.7 ± 4.2 pM. The ATP concentration in superfusate dramatically increased upon switching the solution from isotonic to hypotonic while keeping the rate of fluid flow constant. Figure 11A shows the result of such experiment. After an initial peak (33.7 ± 8.9 times of the basal level), the ATP content in superfusate dropped down to a sustained level of app. 3 times of basal level. Returning the tonicity of the superfusate to normal led to recovery of the ATP in superfusate close to the basal level.

In order to create chemical ischemic conditions, I i) suppressed glycolysis by removing glucose from Ringer solution and including 2-deoxy-D-glucose (10 mM) and ii) blocked the oxidative phosphorylation by 5 mM NaCN. In these conditions, the ATP level of superfusate also exhibited a transient increase. The initial peak value however was not as prominent as for hypotonic stimulation and reached only 4.1 ± 0.8 times of the basal level. Followed the peak, the ATP level remained at sustained level of app. 1.7 times of basal and recovered down to normal level only when the cells were superfused with normal glucose-containing Ringer solution.

It is known that after releasing, ATP rapidly degrades to ADP, AMP and adenosine by ecto-ATPases (Guy Vassort, 2001; Forrester & Williams, 1977; Mathias *et al.* 1991). In my second approach, in order to detect the local concentrations of released ATP in neonatal rat cardiomyocytes upon hypotonic and ischemic conditions, I used a biosensor technique (Hazama *et al.* 1998) based on measuring ATP-evoked ionic currents in PC12 cells that abundantly express P2X receptors on their plasma membrane. Figure 12A shows the current responses to puff applications of 100, 10, and 1 μ M ATP to a PC12 cell, at a holding potential of -50 mV. The concentration-response curve of ATP-induced peak inward current normalized by membrane capacitance is shown in Fig. 12B. The ATP induced currents were detectable at concentrations greater than 1 μ M with a half-maximal concentration of 30.4 ± 2.9 μ M, which is close to the previously reported value of 24.5 μ M (Hazama *et al.* 1998).

When voltage-clamped (at -50 mV) PC12 cell was placed very close to a cardiomyocyte, series of inward current spikes appeared after variable period of time (Fig. 13A, a and b) upon hypotonic stimulation ($n=13$). No inward current spikes were observed when PC12 cell alone was subjected to hypotonic solution (Fig.13A, c; $n=6$). Inward current spikes disappeared when hypotonic solution was supplemented with suramin (300 μ M), a P2 receptor blocker and an ATP scavenger, apyrase (0.1 mg/ml) (Fig. 13A, a and b; $n=4-5$). Pretreatment with these blockers completely abolished the hypotonicity-induced ATP-spikes (Fig.13B, a and b; $n=3-5$). Fig. 13C summarizes the averaged maximal current responses of PC12 cells before and after application of suramin and apyrase in experiments same as shown in Fig. 13A.

Similar inward current spikes were observed when PC12 cells were brought to single cardiomyocytes in conditions of chemical ischemia (Fig.14A, a and b; $n=10$), but not in control condition (Fig.14A, c; $n=8$). Inward current spikes disappeared when

ischemic solution was supplemented with suramin (300 μ M), a P2 receptor blocker and an ATP scavenger, apyrase (0.1 mg/ml) (Fig. 14A, a and b; n=4). Pretreatment with these blockers completely abolished the ischemia-induced ATP-spikes (Fig. 14B, a and b; n=5-6). Fig. 14C summarizes the averaged maximal current responses of PC12 cells before and after application of suramin and apyrase in experiments similar to those shown in Fig. 14A.

Using mean values of current spikes (Figures 13C and 14C) and dose-response curve shown in Fig. 12B I attempted to estimate the magnitude of local ATP concentration rise in my experiments. Hypotonicity-induced inward current density of 8.1 pA/pF corresponds to a local ATP concentration of 22 μ M, and ischemia-induced inward current density of 9.1 pA/pF corresponds to a local ATP concentration of 26.8 μ M. These estimates are upper limits because only maximal current spike amplitude was used in Figures 13C and 14C. My data suggest that upon cell swelling and in ischemic conditions, the local ATP concentration can reach micromolar level that is sufficient to activate most of purinergic cell signaling pathways.

Hypotonicity and ischemic condition activate large conductance channels in cardiomyocytes

The two independent approaches used in my experiments clearly demonstrate that cardiac myocytes possess the ATP-releasing machinery, which can be activated by hypotonic stimulation and in ischemic conditions. We have previously demonstrated that large conductance anion channel (termed VDACL, or Volume-dependent ATP-conducting Large conductance) is involved in swelling-activated ATP release from C127 mouse mammary cells (Sabirov *et al.* 2001; Dutta *et al.* 2002). Here I test the hypothesis that the same channels is involved in swelling- and chemical ischemia-induced ATP release in cardiac myocytes.

Single maxi-Cl channel activity was rarely found in isotonic condition in cell-attached patches. In contrast, when isotonic bath solution was replaced with hypotonic, I observed the activation of single channels with large amplitude after a lag period of 5.7 ± 2.1 min (Fig. 15; n=11). These channels had single-channel amplitude of 11.7 ± 0.82 pA (n=8) and 5.2 ± 0.5 pA (n=10) at holding potentials of +25 mV and -25 mV, respectively. The unitary i-V relationship was slightly outwardly rectifying (presumably due to a lower Cl⁻ concentration within the cell) with a slope conductance

of 359 ± 12 pS at positive voltages and 274 ± 20 pS at negative voltages, and the reversal potential was around -8 mV (Fig.15C, open circles).

When I applied chemical ischemic conditions (same as those used for ATP-release experiment), I also observed single channel events of large amplitude in cardiomyocytes in cell-attached patch configuration. The channel activity appeared after a lag period of 8.4 ± 2.9 min (n=15). The channels (Fig. 16B) had single-channel amplitude of 10.3 ± 0.7 pA (n=19) and 6.8 ± 0.5 pA (n=22) at $+25$ mV and -25 mV, respectively. The unitary i-V relationship was slightly outwardly rectifying with a slope conductance of 390 ± 16 pS at positive voltages and 312 ± 21 pS at negative voltages, and the reversal potential of around 6.6 mV (Fig.16C open circles).

In inside-out mode in normal Ringer solution, the i-V relationship of these maxi-Cl channels was symmetrical and linear (Fig. 16C, closed circles) with slope conductance of 393 ± 4 pS.

Biophysical properties of maxi-Cl channel in cardiomyocytes are similar to VDACL in C127 cells.

Similar to our previous observation in C127 cell (Sabirov *et al.* 2001; Dutta *et al.* 2002), the macromatches excised from cardiac myocytes and containing several maxi-Cl channels demonstrated voltage- and time-dependent inactivation at positive and negative voltages (Fig.17A). The shape of instantaneous current-voltage relationship (Fig.17B, open circles) was close to linear, whereas the steady-state current displayed portions with “negative resistance” at potentials greater than $+20$ and less than -30 mV (Fig.17B, closed circles).

Neither the shape of i-V relationship nor the reversal potential changed when monovalent cations in the bath were replaced with NMDG⁺ (Fig. 17C, closed circles) and in the pipette with TEA⁺ (Fig. 17C, closed squares). In contrast, replacement of chloride with glutamate in the bathing solution shifted the reversal potential to more negative value of -33.8 ± 1.5 mV, (Fig. 17D, closed circles). The calculated permeability ratio of $P_{\text{glutamate}}/P_{\text{Cl}}$ was 0.21 ± 0.02 . Thus, the voltage-dependent gating and anion selectivity of maxi-Cl channels detected in cardiac myocytes are close to that of ATP-releasing VDACL channel in C127 cells (Sabirov *et al.* 2001; Dutta *et al.* 2002).

Cardiac maxi-Cl channel is ATP permeable

In order to function as ATP-releasing channel, the large-conductance channel found in cardiac myocytes must conduct ATP. To verify this, I replaced all anions in the bath solution with 100 mM ATP⁴⁻. In these conditions, the current amplitude of an inside-out patch containing several large-conductance channels was lower than in normal Ringer bath and the I-V relationship became outwardly rectifying (Fig. 18A) and reversed at -14.8 ± 1.7 mV (n=5). Large outward currents (carried by Cl⁻ ions from pipette) and smaller inward currents (carried by ATP⁴⁻ from the bath) could be detected both under ramp clamp (Fig. 18A) and by applying step pulses (Fig. 18B). There is a possibility that these inward currents could be due to entry of Na⁺ from pipette to bath. However, since I detected the same inward currents with very close reversal potential (-16.9 ± 2.1 mV; n=5) when the Na⁺ in pipette was replaced with TEA⁺, I conclude that the inward currents shown in Fig. 18 are ATP-currents. The calculated permeability ratio $P_{\text{ATP}}/P_{\text{Cl}}$ of 0.109 ± 0.014 (normal Ringer in the pipette) and 0.096 ± 0.015 (TEA-pipette solution) was close to the value obtained for VDACL channel in C127 cells (Sabirov *et al.* 2001).

Thus it is concluded that the large-conductance anion channel identified in cardiac myocytes represents ATP-releasing VDACL channel.

Pharmacological profile of cardiac VDACL channel resembles that of ATP release from cardiomyocytes

Figure 19 A and B illustrate the pharmacological profile of the cardiac large-conductance anion channel at the single-channel level. A conventional Cl⁻ channel blocker, SITS (100 μ M), produced profound flickery open-channel block (Fig. 19 A, b). Prominent decrease in single-channel amplitude was observed in the presence of 100 μ M NPPB (Fig. 19 A, c). Arachidonic acid (20 μ M), a potent inhibitor of VDACL channel in C127 cells (Dutta *et al.* 2002) completely abolished the cardiac large-conductance channel activity (Fig. 19, d). The channel was readily blocked by bath application of 50 μ M Gd³⁺ in outside-out (Fig. 19 A, e), but not in inside-out patches (data not shown). The cardiac large-conductance anion single-channel was insensitive to glibenclamide (200 μ M), a potent inhibitor of CFTR and volume-sensitive outwardly

rectifying Cl-channel (Fig. 19 A, f). Mean macropatch currents in the presence of these drugs are summarized in Fig. 19B.

Qualitatively same pharmacological profile was observed in case of ATP-release measurements, where NPPB (100 μ M), SITS (100 μ M), Gd^{3+} (50 μ M) and arachidonic acid (20 μ M) inhibited the swelling-induced ATP release from primary culture of neonatal rat cardiomyocytes. At the same time, glibenclamide (200 μ M), which was ineffective on large-conductance channel activity, also failed to inhibit swelling-induced ATP release from neonatal rat cardiomyocytes significantly (Fig. 19 C).

ATP release and channel activity in hypoxic conditions

Hypoxia is known to induce ATP release from the heart (Vial *et al.* 1987; Borst and Schrader, 1991; Forrester and Williams, 1977). In my experiments, in order to remove oxygen from the cell environment, I used continuous bubbling of normal Ringer solution with 100% argon gas (see Methods). In these conditions, the ATP concentration in superfusate profoundly increased upon switching the solution from normal to hypoxic at constant rate of fluid flow (Fig. 20 A). In contrast to hypotonic stress and chemical ischemia, the initial peak was not obvious and the ATP content in superfusate remained at high sustained level (of app. 10 times of basal level) during the period of hypoxia. Returning to normal conditions led to recovery of the ATP in superfusate close to the basal level.

Inward current spikes similar to those observed in hypotonic and ischemic conditions were detected when PC12 cells were brought to single cardiomyocytes in conditions of hypoxia (Fig.20B, b; n=9), but not in control condition (Fig.20A, a; n=9). Inward current spikes were absent in the presence of suramin (300 μ M), and apyrase (0.1 mg/ml) (Fig. 20B, c and d; n=3). Fig. 20B, e summarizes the averaged maximal current responses of PC12 cells before and after addition of suramin and apyrase. Hypoxia-induced inward current density of 4.1 pA/pF corresponds to a local ATP concentration of 10 μ M, as estimated from dose-response curve shown in Fig. 12B. These estimates are upper limits because only maximal current spike amplitude was used in Figure 20B, e.

The same maneuver induced large-conductance channel activity in neonatal rat cardiomyocytes. When control bath solution was replaced with hypoxic one, the channel activity was observed after a lag period of 8.1 ± 1.8 min (Fig. 20C, a; $n=11$). However, in contrast to hypotonic and chemical ischemic condition, in addition to the full-amplitude VDACL channel with outward current amplitude of 8.5 ± 0.6 pA ($n=5$) at +25 mV and inward current amplitude of 5.7 ± 0.6 pA ($n=5$) mV at -25 mV, (Fig. 20C, b) we often observed a half-amplitude channel type, which had the outward current amplitude of 4.1 ± 0.3 pA ($n=16$) at +25 mV and inward current amplitude of 2.9 ± 0.2 pA ($n=13$) at -25 mV, respectively (Fig. 20C, c). Careful inspection of current traces in hypotonic and chemical ischemic conditions revealed that although the full-amplitude VDACL channel was predominant, 27% patches in hypotonic stimulation experiments and 28 % of patches in ischemic stimulation experiments contained the events with half-maximal amplitudes. This percentage rose up to 70% in hypoxic condition making half-maximal channel predominant in these experimental conditions.

Figure 21 shows biophysical properties of the half-amplitude channel. Patches containing only half-amplitude events displayed voltage-dependent closings at both positive and negative potentials (Fig. 21A). However, the steady-state I-V relationships did not have portions of "negative conductance" seen for full-amplitude channels (Fig. 21B). Voltage-dependency of the half-amplitude channel events was variable and in many instances we observed normal closings at + and - 50 mV holding potential (Fig. 21C). In excised inside-out patches the single-channel i-V relationship was linear (Fig. 21D, open circles) with slope conductance of 193 ± 3 pS. When bath monovalent cations were replaced by NMDG⁺ the single channel amplitude and reversal potential did not change significantly (Fig. 21D, closed circles). However, replacement of bath chloride with glutamate shifted the reversal potential to the negative value of -32.58 ± 2.37 mV (Fig. 21D, closed triangles). The calculated permeability ratio ($P_{\text{glutamate}}/P_{\text{Cl}} = 0.22 \pm 0.03$) was similar to that of full-amplitude VDACL channel. When all anions in the bath solution were replaced with 100 mM ATP⁴⁻ I detected small inward currents both with normal Ringer and TEA-Ringer solution in the pipette (data not shown). The calculated permeability ratio ($P_{\text{ATP}}/P_{\text{Cl}} = 0.09 \pm 0.01$ with Ringer-pipette and $P_{\text{ATP}}/P_{\text{Cl}} = 0.1 \pm 0.023$ with TEA-pipette) was close to that of full-amplitude VDACL channel. From these results I suggested that the half-amplitude channel represents a sub-conductance state of fully open VDACL channel. Despite smaller single-channel

amplitude, this channel is likely to serve as a major conductive pathway for hypoxia-induced ATP release.

DISCUSSION

Translocation of ATP from the intracellular compartment to the extracellular fluid is a fundamental process that provides the substrate for purinergic autocrine and paracrine cell signaling. Although the physiological importance of this process is well recognized, the cellular mechanisms are poorly understood. Existence of a conductive pathway for ATP release was reported in a number of studies, and CFTR was suggested to be a determinant of this process (Reisin *et al.* 1994; Schwiebert *et al.* 1995; Cantiello *et al.* 1997, 1998; Pasyk & Foskett, 1997; Lader *et al.* 2000). In human epithelial Intestine 407 and mouse mammary C127 cell lines, the pathway of swelling-induced ATP release was shown to be distinct from both CFTR and volume-sensitive outwardly rectifying (VSOR) chloride channels (Hazama *et al.* 1998, 1999, 2000 a, b). In our previous study (Sabirov *et al.* 2001), we demonstrated that C127 cells express a large-conductance anion channel, which was silent under normal conditions but could be activated under hypotonic conditions. Based on pharmacological analysis and ATP⁴⁻ current measurements, we concluded that this volume-dependent ATP-conductive large-conductance (VDACL) anion channel serves as a conductive pathway for swelling-induced ATP release from C127 cells. A similar channel in a previous study of kidney macula densa cells, where the channel was regulated by luminal NaCl and was suggested to mediate the ATP release-dependent tubulo-glomerular feedback mechanism (Bell *et al.* 2000).

Arachidonic acid is an abundant constituent of the cell. The concentration of esterified arachidonate in resting platelets, for instance, was estimated to be as high as 5 mM (Brash, 2001). Free arachidonic acid levels are low in the plasma and cytosol, but can rise upon stimulation to 10 – 100 μ M (Brash, 2001). Although most biologic activities of arachidonic acid occur through its conversion to prostaglandins, leukotriens and other products by the cyclooxygenase, lipoxygenase and monooxygenase pathways (Irvine, 1982; Brash, 2001), arachidonic acid itself is also an important regulator of

amplitude, this channel is likely to serve as a major conductive pathway for hypoxia-induced ATP release.

DISCUSSION

Translocation of ATP from the intracellular compartment to the extracellular fluid is a fundamental process that provides the substrate for purinergic autocrine and paracrine cell signaling. Although the physiological importance of this process is well recognized, the cellular mechanisms are poorly understood. Existence of a conductive pathway for ATP release was reported in a number of studies, and CFTR was suggested to be a determinant of this process (Reisin *et al.* 1994; Schwiebert *et al.* 1995; Cantiello *et al.* 1997, 1998; Pasyk & Foskett, 1997; Lader *et al.* 2000). In human epithelial Intestine 407 and mouse mammary C127 cell lines, the pathway of swelling-induced ATP release was shown to be distinct from both CFTR and volume-sensitive outwardly rectifying (VSOR) chloride channels (Hazama *et al.* 1998, 1999, 2000 a, b). In our previous study (Sabirov *et al.* 2001), we demonstrated that C127 cells express a large-conductance anion channel, which was silent under normal conditions but could be activated under hypotonic conditions. Based on pharmacological analysis and ATP⁴⁻ current measurements, we concluded that this volume-dependent ATP-conductive large-conductance (VDACL) anion channel serves as a conductive pathway for swelling-induced ATP release from C127 cells. A similar channel in a previous study of kidney macula densa cells, where the channel was regulated by luminal NaCl and was suggested to mediate the ATP release-dependent tubulo-glomerular feedback mechanism (Bell *et al.* 2000).

Arachidonic acid is an abundant constituent of the cell. The concentration of esterified arachidonate in resting platelets, for instance, was estimated to be as high as 5 mM (Brash, 2001). Free arachidonic acid levels are low in the plasma and cytosol, but can rise upon stimulation to 10 – 100 μ M (Brash, 2001). Although most biologic activities of arachidonic acid occur through its conversion to prostaglandins, leukotriens and other products by the cyclooxygenase, lipoxygenase and monooxygenase pathways (Irvine, 1982; Brash, 2001), arachidonic acid itself is also an important regulator of

many cellular functions, including cell volume regulation (Lambert, 1987; Kubo & Okada, 1992; Margalit *et al.* 1993; Civan *et al.* 1994; Sanchez-Olea *et al.* 1995; Gosling *et al.* 1996; Mignen *et al.* 1999; Hoffmann, 2000). Arachidonic acid has been shown to upregulate ClC-2 Cl⁻ channels (Tewari *et al.* 2000; Cupoletti *et al.* 2001) but to downregulate VSOR (Kubo & Okada, 1992; Nilius *et al.* 1994; Sakai *et al.* 1996; Gosling *et al.* 1996; Xu *et al.* 1997) and other types of Cl⁻ channels (Anderson & Welsh, 1990; Hwang *et al.* 1990; Zachar & Hurnak, 1994; Riquelme & Parra, 1999; Linsdell, 2000).

In the present study, I demonstrate that arachidonic acid is an effective inhibitor of the VDACL anion channel in C127 cells. This result is consistent with previous observations for maxi-Cl⁻ channels from L6 myoblasts (Zachar & Hurnak, 1994) and large anion channels from human term placenta reconstituted in giant liposomes (Riquelme & Parra, 1999). The K_d value of 4 – 5 μ M obtained here is similar to the values observed for a variety of ion channels (Meves, 1994) and is within the physiological range for arachidonic acid concentrations detected in different cells (Brash, 2001). K_m values of 5 μ M for cyclooxygenase and 3.4 – 28 μ M for lipoxygenases (Needleman *et al.* 1986) also indicate that the arachidonic acid concentration in the range of 5 – 10 μ M is physiologically relevant. Therefore, I conclude that arachidonic acid-mediated regulation of VDACL anion channel function actually takes place under physiological conditions.

Arachidonic acid effectively inhibited whole-cell and outside-out macropatch VDACL currents from the extracellular side, but inside-out patch currents from the intracellular side. However, given rapid, diffusional movement of fatty acids across phospholipid bilayers (Kamp & Hamilton, 1993), it is reasonable that arachidonic acid added to the extracellular fluid can easily reach the intracellular moiety and exert its effect from the intracellular side unless the cytosol is perfused. Consistent with this notion, an impermeable analog, arachidonyl CoA, exerted the inhibitory action only from the intracellular side of inside-out patches. In addition, I did not observe any inhibitory change in VDACL channel activity in inside-out patches, when 20 μ M arachidonic acid was added into the pipette solution (data not shown, $n=10$). This observation is similar to that of Zachar and Hurnak (1994) for maxi-Cl⁻ channels from L6 cells. Taken together with arachidonyl CoA data, it is concluded that the site of arachidonate action exists on the cytosolic side of the VDACL anion channel.

In my experiments, arachidonic acid inhibited VDACL channels in two different ways: (i) channel shutdown (decrease in number of active channels) due to a high-affinity binding with a K_d value of 4 – 5 μM ; and (ii) reduced unitary conductance due to low-affinity binding with a K_d value of 13 – 14 μM . The effects of arachidonic acid were direct and not mediated by downstream metabolic products as evidenced by (i) lack of an effect of inhibitors of arachidonate-metabolizing oxygenases and (ii) similar VDACL inhibition by *cis*-unsaturated fatty acids that could not be substrates for oxygenases. Neither *trans*-unsaturated nor saturated fatty acids affected VDACL currents, indicating the importance of the specific conformation of arachidonate's hydrocarbon chain in its inhibitory effect on the VDACL channel. Removing the negative charge of the carboxyl group either by substitution with hydroxyl (arachidonyl alcohol) or by esterification (arachidonyl methyl ester) completely abolished the inhibitory action of arachidonic acid, suggesting the importance of this charge. The necessity for negative charges is in apparent contradiction with voltage-independence of both unitary conductance reduction and channel shutdown. I propose that the inhibitory arachidonate-binding site is located close to the internal entrance to the VDACL channel pore, where little or no voltage drop occurs. Arachidonate binding to the blocking site situated outside the electric field may lead to voltage-independent reduction of single-channel conductance due to either fast open-channel block or a conformational change of the channel pore.

According to the proposed physiological role for the VDACL channel as a conductive pathway for ATP release (Sabirov *et al.* 2001), arachidonic acid must block not only ATP currents but also mass release of ATP induced by cell swelling. Indeed, small inward currents carried by ATP^{4-} were reversibly inhibited by application of arachidonic acid (Fig. 9). Swelling-induced ATP release was also suppressed by arachidonate (Fig. 10). Since arachidonic acid is constantly consumed by endogenous oxygenases, only partial inhibition by arachidonate was observed when these metabolic pathways were still active in intact nonpatched cells. In whole-cell configuration, constant perfusion of intracellular space with the pipette solution may have allowed more profound suppression of VDACL currents by arachidonate due to an increase in effective concentration of arachidonate by washout or decreased specific activity of oxygenases. Inhibition of arachidonate degradation by a cocktail of specific inhibitors for the oxygenases led to an app. 40% reduction in ATP release, presumably due to

accumulation of arachidonic acid generated endogenously in response to the hypotonic stress (Thoroed *et al.* 1997; Tinel *et al.* 1997; Basavappa *et al.* 1998; Pedersen *et al.* 2000; Hoffmann, 2000). In these conditions, exogenously added arachidonate further suppressed ATP release, though still not completely. The K_d values of 4 – 6 μM were very close to those observed in patch-clamp experiments, providing strong evidence for the involvement of the VDACL channel in swelling-induced ATP release. This idea was further supported by the observation that only *cis*-unsaturated fatty acids (oleic and linoleic), but not *trans*-unsaturated (elaidic) or saturated (palmitic) fatty acids, could noticeably affect both swelling-induced ATP release and VDACL channel activity.

Arachidonic acid failed to completely suppress the mass ATP-release from intact cells even in the presence of inhibitory cocktail, whereas arachidonic acid nearly completely eliminated VDACL currents recorded in the whole-cell or excised patch mode. This discrepancy may be related to a complex regulation of ATP-releasing pathways in intact cells compared to excised patches or cells in the whole-cell mode. Swelling-induced activation of phospholipase A2 was reported to lead to an arachidonate-mediated increase in intracellular Ca^{2+} (Oike *et al.* 1994). On the other hand, a Ca^{2+} -mobilizing mitogen, bombesin, and a Ca-ionophore, A23187, were shown to activate the maxi-Cl channel (Kawahara & Takuwa 1991). Thus, I may suppose that in intact cells, a direct inhibiting effect of arachidonic acid on VDACL channel might be attenuated or even counteracted by the Ca^{2+} -mediated enhancing effect on VDACL activation system. Another possible explanation for the above discrepancy would be that arachidonate at high concentrations can form hydrophobic micelles (see Meves 1994). A residual whole-cell current apparent in the presence of arachidonate (Fig. 1) and an arachidonate-insensitive component of macropatch current in Fig. 2B might represent a non-specific leak induced by the arachidonate micelles. I may suppose that a similar leak can be induced by arachidonate in cell membranes in ATP release experiments and might be responsible for the arachidonate-insensitive component of ATP release. On the other hand, I cannot exclude an alternative possibility that the VDACL channel is not a sole ATP-releasing pathway in C127 cells.

Cell swelling is a strong stimulus for arachidonic acid liberation from membrane phospholipids (Thoroed *et al.* 1997; Tinel *et al.* 1997; Basavappa *et al.* 1998; Pedersen *et al.* 2000; Hoffmann, 2000). However, ATP released simultaneously upon cell swelling can also trigger activation of phospholipase A2 and subsequent arachidonic

acid generation (Zambon *et al.* 2000; Scholz-Pedretti *et al.* 2001; Teixeira *et al.* 2001). Therefore, downregulation of the ATP-releasing VDACL channel may constitute a negative feedback in the coupling mechanism of the two powerful signaling pathways mediated by cytosolic arachidonate and extracellular ATP.

In summary, arachidonic acid at micromolar concentrations was found to directly downregulate both the volume-dependent ATP-conductive large-conductance (VDACL) anion channel and swelling-induced ATP release before being metabolized by oxygenases, in C127 cells. This fact provides new evidence for our previous conclusion that the VDACL anion channel serves as a pathway for swelling-induced ATP release, both being under a negative control by intracellular arachidonic acid signaling.

In resting condition interstitial heart fluid contains a significant amount of ATP, but during ischemia this ATP can increase upto 10 fold or more (Kuzmin *et al.* 1998). The sources of ATP during hypoxia or ischemia/reperfusion are poorly known. The possibilities are; (1) from purinergic nerves (Burnstock, 1972), (2) from vascular endothelial or smooth muscle cells (Pearson & Gordan, 1985; Sparks & Bardenheuer, 1986), (3) ATP release was reported from isolated cardiomyocytes in hypoxic condition (Forrester & Williams, 1977).

In this study, I reported first time that from primary culture of neonatal rat cardiomyocytes, massive release of ATP occurred upon hypotonic, chemical ischemic as well as hypoxic conditions. The kinetics of ATP release was biphasic, a transient peak followed by steady state both in hypotonic and chemical ischemic conditions. The similar result has been noted by Paddle & Burnstock (1974) in guinea-pig heart and by Forrester & Williams (1977) in isolated adult rat cardiomyocytes in hypoxic conditions. Jans *et al.* (2002), observed a similar result in cultured renal epithelial cells (A6), basolateral membrane. Ventricular rhythm disturbances occurred transiently during early period of ischemia when interstitial ATP peaked in the ischemic zone are in accordance with the deleterious arrhythmogenic effects of ATP (Kuzmin *et al.* 1998), agree with fig.1 result. From this result it is reasonable to assume that, during ischemic attack, a large amount of ATP release from cardiomyocytes in interstitial space of coronary tissue.

After releasing, most of the ATP are degraded rapidly to ADP>AMP>Adenosine by ecto-ATPase, ecto-ADPase and ecto-5'-nucleotidase (Kuzmin *et al.* 1998; Vassort, 2001; Williamson & Dipietro, 1965; Forrester & Williams, 1977; Borst & Schrader, 1991) and exerts its physiological function. ATP degradation rate is over 95% during a single coronary passage (Vassort, 2001). I provided evidence that local concentration of ATP in ischemic, hypoxic and hypotonic conditions exceed micromolar levels sufficient to activate P2-purinergic receptors, presented on sarcolemma (Vassort, 2001) detected by biosensor technique (Hazama *et al.* 1998). This result further supported the idea that, a large amount of the ATP released in the interstitial space of coronary tissue, upon hypotonic, ischemic as well as hypoxic conditions were from cardiomyocytes.

The physiological and pathological roles of the released ATP in ischemic and hypoxic conditions, are various; such as deleterious in global ischemia/reperfusion but protective in short period of ischemia and hypoxia (Vassort, 2001; Cohen *et al.* 2000; Ninomiya *et al.* 2002; Kuzmin *et al.* 1998), but the cellular mechanisms of ATP release from cardiomyocytes are obscured.

I observed activity of ATP releasing machinery, VDACL channel in cardiomyocytes, in cell-attached patch configuration, like C127 cells (Sabirov *et al.* 2001), in same pathophysiological conditions, those induced ATP release. A similar channel activity was observed in newborn rat in hypotonic media or after formation of bleb by Coulombe & Coraboeuf (1992) in cell-attached patch mode. The biophysical properties of cardiac VDACL channel are similar to VDACL channel present in C127 cells, for instance voltage- and time-dependent inactivation at larger potentials as well as anion selectivity (fig.17). I could record ATP conducting currents from neonatal rat cardiomyocytes, in an inside-out patch (fig.18), like ATP conducting currents in C127 cells (Sabirov *et al.* 2001). The pharmacological profile of the cardiac VDACL channel and swelling-induced ATP release are similar in neonatal rat cardiomyocytes, like our previous study in C127 cells (Sabirov *et al.* 2001). Activating mechanism, ATP conducting property as well as qualitatively same pharmacological profile, suggested that cardiac VDACL is also ATP permeable.

The inhibitory effect of arachidonic acid on swelling-induced ATP release was partial but same concentration of arachidonic acid almost completely inhibited cardiac VDACL currents recorded from inside-out patches (fig. 19). The similar result also observed in C127 cells and the effect of arachidonic acid was direct as described before.

Lader *et al.* (2000a,b) observed cAMP activated ATP currents in neonatal rat and mouse cardiomyocytes. The pharmacological property of ATP release and activation of cAMP activated chloride currents are distinct from our present study, for instance glibenclamide which is potent blocker of cardiac CFTR (Lader *et al.* 2000) failed to inhibit hypotonicity induced ATP release as well as VDACL channel activity from primary culture of neonatal rat cardiomyocytes in our present study. On the other hand DIDS failed to inhibit cAMP activated chloride current as well as ATP release from primary culture of neonatal rat cardiomyocytes (Lader *et al.* 2000) but SITS in our present study, inhibited both VDACL channel and hypotonicity induced ATP release from primary culture of neonatal rat cardiomyocytes. So my data suggested that cAMP activated and swelling-induced ATP release pathway might be distinct.

Maxi-Cl⁻ channel functionally expressed in various types of cells; (1) Human T lymphocytes (Schlichter *et al.* 1990; Pahapill *et al.* 1992) (2) Endothelial cell (Olesen & Bundgaard. 1992; Li *et al.* 1999; Groschner & Kukovetz 1992) (3) Epithelial cell (Schwiebert *et al.* 1990; 1994 Dietl & Stanton 1992; Mitchel *et al.* 1997; McGill *et al.* 1993) (4) Tumor cell lines (Vaca & Kunze 1992; Falke & Misler 1989) (5) Astrocytic cell line (Guibert *et al.* 1998; Jalonen, 1993) (6) Muscle cell (Blatz & Magleby 1983; Sun *et al.* 1992; 1993) (7) C1300 mouse neuroblastoma cells (Diaz *et al.* 2001) (8) NIH3T3 fibroblasts (Valverde *et al.* 2002) and (10) From our laboratory C127, mammary cell line (Sabirov *et al.* 2001), Kidney macula-densa cell (Bell *et al.* 2000). At present the physiological importance of this channel is obscure, although the activation and regulation of this channel differs from cell to cell.

In summary, cell-swelling induced massive release of ATP as well as VDACL channel activation both in C127 mouse mammary cell line and primary culture of neonatal rat cardiomyocytes. Pathophysiological conditions like ischemia as well as hypoxia induced massive release of ATP from primary culture of neonatal rat cardiomyocytes. Same stimuli known to activate PLA₂, resulting in generation of arachidonic acid. Arachidonic acid regulated VDACL channel by two different ways, (1) Reduction of unitary conductance and (2) Channel shutdown.

Ischemic preconditioning is a phenomenon whereby exposure of the myocardium to a brief episode of ischemia and reperfusion markedly reduces tissue necrosis induced by a subsequent prolonged ischemia. In these receptors mediated processes, not only adenosine but also ATP itself may play an essential role (Ninomiya *et al.* 2002).

Arachidonic acid which inhibited ATP release as well as VDACL channel activity in primary culture of neonatal rat cardiomyocytes, known to release upon ischemic and hypoxic conditions, through a pathway involving PLA2 (Mchowat *et al.* 1998; Michiels *et al.* 2002). This released arachidonic acid protect neonatal rat cardiomyocytes from ischemic injury through PKC ϵ (Mackay & Mochly-Rosen, 2001). A membrane-associated iPLA2 activity was also increased by PKC ϵ (Steer *et al.* 2002). More over free polyunsaturated fatty acids like arachidonic acid prevent arrhythmias (a pathophysiological symptom usually occur during myocardial ischemia) in neonatal rat cardiomyocytes (Kang & Leaf, 1995). Ventricular rhythm disturbances occurred during early period of ischemia due to peaked ATP level (Kuzmin *et al.* 1998). So inhibitory effect of ATP release by arachidonic acid, could suppress arrhythmogenic effects of ATP during ischemic attack.

ACKNOWLEDGMENTS

I am very grateful to Prof. Yasunobu Okada and Associate Prof. Ravshan Z. Sabirov for their guidance and support throughout my study. I would like to thank Dr. Shigeru Morishima and Hiromi Uramoto for teaching Cardiomyocytes isolation and primary culture techniques. I am also grateful to K. Shigemoto, S. Sabirova, M. Ohara for their technical supports and T. Okayasu for secretarial assistance. And I like to thank all members of our laboratory for well co-operation and generous support.

REFERENCES

ABRAHAM, E.H., PRAT, A.G., GERWECK, L., SENEVERATNE, T., ARCECI, R.J., KRAMER, R., GUIDOTTI, G. & CANTIELLO, H.F. (1993). The multidrug resistance (*mdr1*) gene product functions as an ATP channel. *Proceedings of the National Academy of Sciences of the USA* **90**, 312-316.

ANDERSON, M.P. & WELSH, M.J. (1990). Fatty acids inhibit apical membrane chloride channels in airway epithelia. *Proceedings of the National Academy of Sciences of the USA* **87**, 7334-7338.

BASAVAPPA, S.S., PEDERSEN, F., JORGENSEN, N.K., ELLORY, J.C. & HOFFMANN, E.K. (1998). Swelling-induced arachidonic acid release via the 85-kDa cPLA₂ in human neuroblastoma cells. *Journal of Neurophysiology* **79**, 1441-1449.

BELL, P.D., LAPOINTE, J.-Y., SABIROV, R., HAYASHI, S. & OKADA, Y. (2000). Maxi-chloride channel in macula densa cells: possible pathway for ATP release. *FASEB Journal* **14**, A134. (Abstr.)

BLATZ, A. L. & MAGLEBY, K. L. (1983). Single voltage-dependent chloride-selective channels of large conductance in cultured rat muscle. *Biophysical Journal* **43**, 237-241.

BLONDEL, B. ROIJEN, I. & CHENEVAL, J.P. (1971). Heart cells in culture: a simple method for increasing the proportion of myoblasts. *Experientia* **27**, 356-358.

BODAS, E., ALEU, J., PUJOL, G., MARTIN-SATUE, M., MARSAL, J. & SOLSONA, C. (2000). ATP crossing the cell plasma membrane generates an ionic current in *Xenopus* oocytes. *Journal of Biological Chemistry* **275**, 20268-20273.

BODIN, P. & BURNSTOCK, G. (2001). Purinergic signalling: ATP release. *Neurochemical research* **26**, 959-969.

BORST, M.M & SCHRADER, J. (1991). Adenosine nucleotide release from isolated perfused guinea pig hearts and extracellular formation of adenosine. *Circulation Research* **68**, 797-806.

BOUDREAULT, F. & GRYGORCZYK, R. (2002). Cell swelling-induced ATP release and gadolinium-sensitive channels. *American Journal of Physiology* **282**, C219-C226.

BOSCH, I., JACKSON, G.R. JR., CROOP, J.M. & CANTIELLO, H.F. (1996). Expression of *Drosophila melanogaster* P-glycoproteins is associated with ATP channel activity. *American Journal of Physiology* **271**, C1527-C1538.

BRASH, A.R. (2001). Arachidonic acid as a bioactive molecule. *The Journal of Clinical Investigations* **107**, 1339-1345.

BURNSTOCK, G. (1999). Release of vasoactive substances from endothelial cells by shear stress and purinergic mechanosensory transduction. *Journal of Anatomy* **194**, 335-342.

BURNSTOCK, G. (1972). Purinergic nerves. *Pharmacological Review* **24**, 509-581.

BURNSTOCK, G. & KENNEDY, C. (1986). Purinergic receptors in the cardiovascular system. *Prog Pharmacol* **6**: 111-132, 1986.

CANTIELLO, H.F., JACKSON, G.R. JR., PRAT, A.G., GAZLEY, J.L., FORREST, J.N. JR. & AUSIELLO, D.A. (1997). cAMP activates an ATP-conductive pathway in

cultured shark rectal gland cells. *American Journal of Physiology* **272**, C466-C475.

CANTIELLO, H.F., JACKSON, G.R. JR., GROSMAN, C.F., PRAT, A.G., BORKAN, S.C., WANG, Y., REISIN, I.L., O'RIORDAN, C.R. & AUSIELLO, F.A. (1998). Electrodifusional ATP movement through the cystic fibrosis transmembrane conductance regulator. *American Journal of Physiology* **274**, C799-C809.

CIVAN, M.M, COCA-PRADOS, M. & PETERSON-YANTORNO, K. (1994). Pathways signaling the regulatory volume decrease of cultured nonpigmented ciliary epithelial cells. *Investigative ophthalmology & visual science* **35**, 2876-2886.

COADE, S.B. & PEARSON, J.D. (1989). Metabolism of adenine nucleotides in human blood. *Circulation Research* **65**, 531-537.

COHEN, M.V., BAINES, C.P. & DOWNEY, J.M. (2000). Ischemic preconditioning: from adenosine receptor to K_{ATP} channel. *Annual Review of Physiology* **62**, 79-109.

COULOMBE, A. & CORABOEUF, E. (1992). Large-conductance chloride channels of new-born rat cardiac myocytes are activated by hypotonic media. *Pfugers Arch* **422**, 143-150.

CUPPOLETTI, J., TEWARI, K.P., SHERRY, A.M., KUPERT, E.Y. & MALINOWSKA, D.H. (2001). ClC-2 Cl⁻ channels in human lung epithelia: activation by arachidonic acid, amidation, and acid-activated omeprazole. *American Journal of Physiology* **281**, C46-C54.

DENSON, D.D., WANG, X., WORRELL, R.T. & EATON, D.C. (2000). Effects of fatty acids on BK channels in GH(3) cells. *American Journal of Physiology* **279**, C1211-C1219.

DIAZ, M., BAHAMONDE, M.I., LOCK, H., MUNOZ, F.J., HARDY, S.P., POSAS, F. & VALVERDE, M.A. (2001). Okadaic acid-sensitive activation of Maxi Cl⁻ channels by triphenylethylene antioestrogens in C1300 mouse neuroblastoma cells. *Journal of Physiology* **536**, 79-88.

DIETL, P. & STANTON, B. A. (1992). Chloride channels in apical and basolateral membranes of CCD cells (RCCT-28A) in culture. *American Journal of Physiology- Renal Fluid Electrolyte Physiology* **263**, F243-F250.

DUTTA, A.K, OKADA, Y. & SABIROV, R.Z. (2002). Regulation of an ATP-conductive large-conductance anion channel and swelling-induced ATP release by arachidonic acid. *Journal of Physiology* **542**, 803-816.

FALKE, L. C. & MISLER, S. (1989). Activity of ion channels during volume regulation by clonal N1E115 neuroblastoma cells. *Proceedings of the National Academy of Sciences of the USA* **86**, 3919-3923.

FAN, H.T., MORISHIMA, S., KIDA, H. & OKADA, Y. (2001). Phloretin differentially inhibits volume-sensitive and cyclic AMP-activated, but not Ca-activated, Cl⁻ channels. *British Journal of Pharmacology* **133**, 1096-1106.

FORRESTER, T. & WILLIAMS, C. A. (1977). Release of adenosine triphosphate from isolated adult heart cells in response to hypoxia. *Journal of Physiology* **268**, 371-390.

FERANCHAK, A.P., ROMAN, R.M., SCHWIEBERT, E.M. & FITZ, J.G. (1998). Phosphatidylinositol 3-kinase contributes to cell volume regulation through effects on ATP release. *Journal of Biological Chemistry* **273**, 14906-14911.

GOSLING, M., POYNER, D.R. & SMITH, J.W. (1996). Effects of arachidonic acid upon the volume-sensitive chloride current in rat osteoblast-like (ROS 17/2.8) cells. *Journal of Physiology* **493**: 613-623.

GROSCHNER, K. & W.R., KUKOVETZ. (1992). Voltage-sensitive chloride channels of large conductance in the membrane of pig aortic endothelial cells. *Pfugers Arch* **421**, 209-217.

GUIBERT, B., DERMETZEL, R. & SIEMEN, D. (1998). Large conductance channel in plasma membranes of astrocytic cells is functionally related to mitochondrial VDAC-channels. *The International Journal of Biochemistry and Cell Biology* **30**, 379-391.

GRYGORCZYK, R. & HANRAHAN, J.W. (1997). CFTR-independent ATP release from epithelial cells triggered by mechanical stimuli. *American Journal of Physiology* **272**, C1058-C1066.

HAZAMA, A., HAYASHI, S. & Y. OKADA, Y. (1998). Cell surface measurements of ATP release from single pancreatic β cells using a novel biosensor technique. *Pfugers Arch* **437**, 31-35.

HAZAMA, A., MIWA, A., MIYOSHI, T., SHIMIZU, T. & OKADA, Y. (1998). ATP release from swollen or CFTR-expressing epithelial cells. In *Cell Volume Regulation: The Molecular Mechanism and Volume Sensing Machinery*, ed. Okada, Y., pp. 93-98. Elsevier, Amsterdam.

HAZAMA, A., SHIMIZU, T., ANDO-AKATSUKA, Y., HAYASHI, S., TANAKA, S., MAENO, E. & OKADA, Y. (1999). Swelling-induced, CFTR-independent ATP release from a human epithelial cell line: lack of correlation with volume-sensitive Cl^- channels. *Journal of General Physiology* **114**, 525-533.

- HAZAMA, A., ANDO-AKATSUKA, Y., FAN, H.-T., TANAKA, S. & OKADA, Y. (2000a). CFTR-dependent and -independent ATP release induced by osmotic swelling. In *Control and Disease of Sodium Dependent Transportation Proteins and Ion Channels*. eds. Suketa, Y., Carafoli, E., Lazduski, M., Mikoshiba, K., Okada, Y. & Wright, E.M., pp. 429-431. Elsevier, Amsterdam.
- HAZAMA, A., FAN, H.-T., ABDULLAEV, I., MAENO, E., TANAKA, S., ANDO-AKATSUKA, Y. & OKADA, Y. (2000b). Swelling-augmented ATP release and Cl^- conductances in murine C127 cells. *Journal of Physiology* **523**, 1-11.
- HOFFMANN, E.K. (2000). Intracellular signaling involved in volume regulatory decrease. *Cellular physiology and biochemistry* **10**, 273-288.
- HOLTZMAN, M.J. (1991). Arachidonic acid metabolism. Implications of biological chemistry for lung function and disease. *The American Review of Respiratory Disease* **143**, 188-203.
- HOPWOOD, A.M. & BURNSTOCK, G. (1987). ATP mediates coronary vasoconstriction via $\text{P}_{2\text{x}}$ -purinoceptors and coronary vasodilatation via $\text{P}_{2\text{y}}$ -purinoceptors in the isolated perfused rat heart. *European Journal of Pharmacology* **136**, 49-54.
- HWANG, T.C., GUGGINO, S.E. & GUGGINO, W.B. (1990). Direct modulation of secretory chloride channels by arachidonic and other cis unsaturated fatty acids. *Proceedings of the National Academy of Sciences of the USA* **87**, 5706-5709.
- JALONEN, T. (1993). Single-channel characteristics of the large-conductance anion channel in rat cortical astrocytes in primary culture. *Glia* **9**, 227-237.
- JANS, D., SRINIVAS, S.P., WAELEKENS, E., SEGAL, A., LARIVIERE, E., SIMAELS, J. & VAN DRIESCHE, W. (2002). Hypotonic treatment evokes biphasic ATP

release across the basolateral membrane of cultured renal epithelia(A6). *Journal of Physiology* **545**, 543-555.

IRVINE, R.F. (1982). How is the level of free arachidonic acid controlled in mammalian cells? *The Biochemical Journal* **204**, 3-16.

KAMP, F. & HAMILTON, J.A. (1993). Movement of fatty acids, fatty acid analogues, and bile acids across phospholipid bilayers. *Biochemistry* **32**, 11074-11086.

KANG, J.X. & LEAF, A. (1995). Prevention and termination of β -adrenergic agonist-induced arrhythmias by free polyunsaturated fatty acids in neonatal rat cardiac myocytes. *Biochemical and Biophysical Research Communications* **208**, 629-636.

KAWAHARA, K. & TAKUWA, N. (1991). Bombesin activates large-conductance chloride channels in Swiss 3T3 fibroblasts. *Biochemical and Biophysical Research Communications* **177**, 292-298.

KUBO, M. & OKADA, Y. (1992). Volume-regulatory Cl^- channel currents in cultured human epithelial cells. *Journal of Physiology* **456**, 351-371.

KUZMIN, A. I., GOURINE, A.V., MOLOSH, A.I., LAKOMKIN, V. L. & VASSORT, G. (1998). Interstitial ATP level and degradation in control and postmyocardial infarcted rats. *American Journal of Physiology- Cell Physiol* **275**, C766-C771.

KUZMIN, A. I., KAPELKO V. I., LAKOMKIN V. L. & VASSORT, G. (2000). Effects of preconditioning on myocardial interstitial levels of ATP and its catabolites during regional ischemia and reperfusion in the rat. *Basic Research of Cardiology* **95**, 127-136.

LADER, A.S., XIAO, Y.F., O'RIORDAN, C.R., PRAT, A.G., JACKSON, G.R. JR. & CANTIELLO, H.F. (2000). cAMP activates an ATP-permeable pathway in neonatal rat cardiac myocytes. *American Journal of Physiology* **279**, C173-C187.

LADER, A.S., WANG, Y., JACKSON, G.R. JR., BORKAN, S.C. & CANTIELLO, H.F. (2000). cAMP-activated anion conductance is associated with expression of CFTR in neonatal mouse cardiac myocytes. *American Journal of Physiology-Cell Physiology* **278**, C436-C450.

LAMBERT, I. H. (1987). Effect of arachidonic acid, fatty acids, prostaglandins and leukotrienes on volume regulation in Ehrlich ascites tumor cells. *Journal of Membrane Biology* **98**, 207-221.

LEVESQUE, P.C. & HUME, J.R. (1995). ATP_o but not cAMP_i activates a chloride conductance in mouse ventricular myocytes. *Cardiovascular Research* **29**, 336-343.

LI, Z., NIWA, Y., SAKAMOTO, S., CHEN, X. & NAKAYA, Y. (1999). Estrogen modulates a large conductance chloride channel in cultured porcine aortic endothelial cells. *Journal of Cardiovascular Pharmacology* **35**, 506-510.

LIGHT, D.B., CAPES, T.L., GRONAU, R.T. & ADLER, M.R. (1999). Extracellular ATP stimulates volume decrease in Necturus red blood cells. *American Journal of Physiology-cell physiology* **277**, C480-C491.

LINDELL, P. (2000). Inhibition of cystic fibrosis transmembrane conductance regulator chloride channel currents by arachidonic acid. *Canadian Journal of Physiology and Pharmacology* **78**, 490-499.

MACKAY, K. & MOCHLY-ROSEN, D. (2001). Arachidonic acid protects neonatal rat cardiac myocytes from ischemic injury through ϵ protein kinase C. *Cardiovascular Research* **50**, 65-74.

MARGALIT, A., LIVNE A.A, FUNDER J. & GRANOT, Y. (1993). Initiation of RVD response in human platelets: mechanical-biochemical transduction involves pertussis-toxin-sensitive G protein and phospholipase A₂. *Journal of Membrane Biology* **136**, 303-311.

McGILL, J.M., GETTYS, T.W., BASAVAPPA, S. & FITZ, J.G. (1993). GTP-binding proteins regulate high conductance anion channels in rat bile duct epithelial cells. *Journal of Membrane Biology* **133**, 253-261.

McHOWAT, J., LIU, S. & CREER, M.H. (1998). Selective hydrolysis of plasmalogen phospholipids by Ca²⁺-independent PLA₂ in hypoxic ventricular myocytes. *American Journal of Physiology-cell physiology* **274**, C1727-C1737.

MEVES, H. (1994). Modulation of ion channels by arachidonic acid. *Progress in Neurobiology* **43**, 175-186.

MICHIELS, C., RENARD, P., BOUAZIZ, N., HECK, N., ELIAERS, F., NINANE, N., QUARCK, R., HOLVOET, P. & RAES, M. (2002). Identification of phospholipase A₂ isoforms that contribute to arachidonic acid release in hypoxic endothelial cells: limits of phospholipase A₂ inhibitors. *Biochemical Pharmacology* **63**, 321-332.

MIGNEN, O., LE GALL, C., HARVEY, B.J. & THOMAS, S. (1999). Volume regulation following hypotonic shock in isolated crypts of mouse distal colon. *Journal of Physiology* **515**, 501-510.

MITCHELL, C.H., WANG, L. & JACOB, T.J.C. (1997). A large-conductance chloride channel in pigmented ciliary epithelial cells activated by GTP γ S. *Journal of Membrane Biology* **158**, 167-175.

MITCHELL, C.H., CARRE, D.A., MCGLINN, A.M., STONE, R.A. & CIVAN, M.M. (1998). A release mechanism for stored ATP in ocular ciliary epithelial cells. *Proceedings of the National Academy of Sciences of the USA* **95**, 7174-7178.

NEEDLEMAN, P., TURK, J., JAKSCHIK, B.A., MORRISON, A.R. & LEFKOWITH, J.B. (1986). Arachidonic acid metabolism. *Annual Review of Biochemistry* **55**, 69-102.

NINOMIYA, H., OTANI, H., LU, K., UCHIYAMA, T., KIDO, M. & IMAMURA, H. (2002). Complementary role of extracellular ATP and adenosine in ischemic preconditioning in the rat heart. *American Journal of Physiology- Heart Circulatory Physiology* **282**, H1810-H1820.

NILIUS, B., OIKE, M., ZAHRADNIK, I. & DROOGMANS, G. (1994). Activation of a Cl⁻ current in hypotonic volume increase in human endothelial cells. *Journal of General Physiology* **103**, 787-805.

OIKE, M., DROOGMANS, G. & NILIUS, B. (1994). Mechanosensitive Ca²⁺ transients in endothelial cells from human umbilical vein. *Proceedings of the National Academy of Sciences of the USA* **91**, 2940-2944.

OLESEN, S. P. & BUNDGAARD, M. (1992). Chloride-selective channels of large conductance in bovine aortic endothelial cells. *Acta Physiological Scand* **144**, 191-198.

PADDLE, B. M. & BURNSTOCK, G. (1974). Release of ATP from perfused heart during coronary vasodilatation. *Blood Vessels* **11**, 110-119

PAHAPILL, P. A. & SCHLICHTER, L. C. (1992). Cl⁻ Channels in intact human T lymphocytes. *Journal of Membrane Biology* **125**, 171-183.

PASYK, E.A. & FOSKETT, J.K. 1997. Cystic fibrosis transmembrane conductance regulator-associated ATP and adenosine 3'-phosphate 5'-phosphosulfate channels in endoplasmic reticulum and plasma membranes. *Journal of Biological Chemistry* **272**, 7746-7751.

PEARSON, J. D. & GORDON, J. L. (1985). Nucleotide metabolism by endothelium. *Ann Res Physiol* **47**, 617-627.

PEDERSEN, S., LAMBERT, I.H., THOROED, S.M. & HOFFMANN, E.K. 2000. Hypotonic cell swelling induces translocation of the alpha isoform of cytosolic phospholipase A2 but not the gamma isoform in Ehrlich ascites tumor cells. *European Journal of Biochemistry* **267**, 5531-5539.

PELLEG, A., HURT, C. M. & MICHELSON, E. L. (1990). Cardiac effects of adenosine and ATP. In: *Biological Actions of Extracellular ATP*, edited by Dubyak GR and Fedan JS. New York: *NY Academy of Sciences*, p. 19-30.

QU, Y., HIMMEL, H. M., CAMPBELL, D. L. & STRAUSS, H. C. (1993). Effects of extracellular ATP on I_{Ca} , $[Ca^{2+}]_i$, and contraction in isolated ferret ventricular myocytes. *American Journal of Physiology- Cell Physiology* **264**, C702-C708.

RAINSFORD, K.D. 1988. Inhibitors of eicosanoid metabolism. In *Prostaglandins: Biology and Chemistry of prostaglandins and Related Eicosanoids*. P.B. ed. Curtis-Prior, pp. 52-68, Churchill Livingstone, Edinburgh.

REISIN, I.L., PRAT, A.G., ABRAHAM, E.H., AMARA, J.F., GRYGORY, R.J., AUSIELLO, D.A. & CANTIELLO, H.F. (1994). The cystic fibrosis transmembrane

conductance regulator is a dual ATP and chloride channel. *Journal of Biological Chemistry* **269**, 20584-20591.

SAKAI, H., KAKINOKI, B., DIENER, M. & TAKEGUCHI, N. (1996). Endogenous arachidonic acid inhibits hypotonically-activated Cl^- channels in isolated rat hepatocytes. *Japanese Journal of Physiology* **46**, 311-318.

SANCHEZ-OLEA, R., MORALES-MULIA, M., MORAN, J. & PASANTES-MORALES, H. (1995). Inhibition by polyunsaturated fatty acids of cell volume regulation and osmolytes fluxes in astrocytes. *American Journal of Physiology* **269**, C96-C102.

SCHOLZ-PEDRETTI, K., PFEILSCHIFTER, J. & KASZKIN, M. (2001). Potentiation of cytokine induction of group IIA phospholipase A_2 in rat mesangial cells by ATP and adenosine via the A_2A adenosine receptor. *British Journal of Pharmacology* **132**, 37-46.

SCAMPS, F. & VASSORT, G. (1994). Effect of extracellular ATP on the Na^+ current in rat ventricular myocytes. *Circulation Research* **74**, 710-717.

SCHLICHTER, L. C., GRYGORCZYK, R., PAHAPILL, P. A. & GRYGORCZYK, C. (1990). A Large, multiple-conductance chloride channel in normal human T lymphocytes. *Pfugers Arch* **416**, 413-421.

SCHWIEBERT, E.K., EGAN, M.E., HWANG, T.-H., FULMER, S.B., ALLEN, S.S., CUTTING, G.R. & GUGGINO, W.B. (1995). CFTR regulates outwardly rectifying chloride channels through an autocrine mechanism involving ATP. *Cell* **81**, 1063-1073.

SHODA, M, HAGIWARA, N., KASANUKI, H. & HOSODA, S. (1997). ATP-activated cationic current in rabbit sino-atrial node cells. *Journal of Molecular and Cellular Cardiology* **29**, 689-695.

SIMPSON, P. & SAVION, S. (1982). Differentiation of rat myocytes in single cell cultures with and without proliferating nonmyocardial cells. *Circulation Research* **50**, 101-116.

SMIRNOV, S.V. & AARONSON, P.I. 1996. Modulatory effects of arachidonic acid on the delayed rectifier K^+ current in rat pulmonary arterial myocytes. Structural aspects and involvement of protein kinase C. *Circulation Research* **79**, 20-31.

SPARKS, H. V. & BARDENHEUER, H. (1986). Regulation of adenosine formation by the heart. *Circulation Research* **58**, 193-201.

STEER, S.A., WIRSIG, K.C., CREER, M.H., FORD, D.A. & MCHOWAT, J. (2002). Regulation of membrane-associated iPLA₂ activity by a novel PKC isoform in ventricular myocytes. *American Journal of Physiology- Cell Physiology* **283**, C1621-C1626.

SUGITA, M., YUE, Y. & FOSKETT, J.K. (1998). CFTR Cl^- channel and CFTR-associated ATP channel: distinct pores regulated by common gates. *EMBO Journal* **17**: 898-908.

SUN, X.P., SUPPLISSON, S., TORRES, R., SACHS, G. & MAYER, E. (1992). Characterization of large-conductance chloride channels rabbit colonic smooth muscle. *Journal of Physiology* **448**, 355-382.

SUN, X.P., SUPPLISSON, S. & MAYER, E. (1993). Chloride channels in myocytes from rabbit colon are regulated by a pertussis toxin-sensitive G protein. *American Journal of physiology* **264**, G774-G785.

TAYLOR, A.L., KUDLOW, B.A., MARRS, K.L., DRUENERT, D.C., GUGGINO, W.B. & SCHWIEBERT, E.M. (1998). Bioluminescence detection of ATP release mechanisms in epithelia. *American Journal of Physiology-Cell Physiology* **275**, C1391-C1406.

TEIXEIRA, M., BERNARD, C., FERRARY, E. & BUTLEN, D. 2001 Purine and pyrimidine nucleotide-sensitive phospholipase A₂ in ampulla from frog semicircular canal. *American Journal of Physiology* **280**: R519-R526.

TEWARI, K.P., MALINOWSKA, D.H., SHERRY, A.M. & CUPPOLETTI, J. (2000). PKA and arachidonic acid activation of human recombinant ClC-2 chloride channels. *American Journal of Physiology* **279**: C40-C50.

THOROED, S.M., LAURITZEN, V., LAMBERT, I.H., HANSEN, H.S. & HOFFMANN, E.K. (1997). Cell swelling activates phospholipase A₂ in Ehrlich ascites tumor cells. *Journal of Membrane Biology* **160**, 47-58.

TINEL, H., WEHNER, F. & KINNE, R.K. (1997). Arachidonic acid as a second messenger for hypotonicity-induced calcium transients in rat IMCD cells. *Pflugers Archiv* **433**, 245-253.

VACA, L. & KUNZE, D. L. (1992). Anion and cation permeability of a large conductance anion in the T84 human colonic cell line. *Journal of Membrane Biology* **130**, 241-249.

VALVERDE, M.A., HARDY, S.P. & DIAZ, M. (2002). Activation of Maxi Cl⁻ channels by antiestrogens and Phenothiazines in NIH3T3 fibroblasts. *Steroids*. **67**(6), 439-45.

VASSORT, G. (2001). Adenosine 5'-Triphosphate: a P2-purinergic agonist in the myocardium. *Physiological Reviews* **81**, 767-806.

VIAL, C., OWEN, P., OPIE L. H. & POSEL, D. (1987). Significance of adenosine triphosphate and adenosine induced by hypoxia or adrenaline in perfused rat heart. *Journal of Molecular Cell Cardiology* **19**, 187-197.

WANG, Y., ROMAN, R., LIDOFKY, S.D. & FITZ, J.G. (1996). Autocrine signaling through ATP release represents a novel mechanism for cell volume regulation. *Proceedings of National Academy of Sciences of the USA*. **93**, 12020-12025.

WILLIAMSON, J. R. & DIPIETRO, D. L. (1965). Evidence for extracellular enzymatic activity of the isolated perfused rat heart. *Biochemical Journal* **95**, 226-232.

XU, W.X., KIM, S.J., SO, I., KANG, T.M., RHEE, J.C. & KIM, K.W. (1997). Volume-sensitive chloride current activated by hyposmotic swelling in antral gastric myocytes of the guinea pig. *Pflugers Archiv* **435**, 9-19.

ZACHAR, J. & HURNAK, O. (1994). Arachidonic acid blocks large-conductance chloride channels in L6 myoblasts. *General Physiology and Biophysics* **13**, 193-213.

ZAMBON, A.C., HUGHES, J.R., MESZAROS, V, WU, V, TORRES, V, BRUNTON, V. & INSEL, P.A. (2000). P2Y₂ receptor of MDCK cells: cloning, expression, and cell-specific signaling. *American Journal of Physiology*. **279**, F1045-F1052.

FIGURES AND LEGENDS

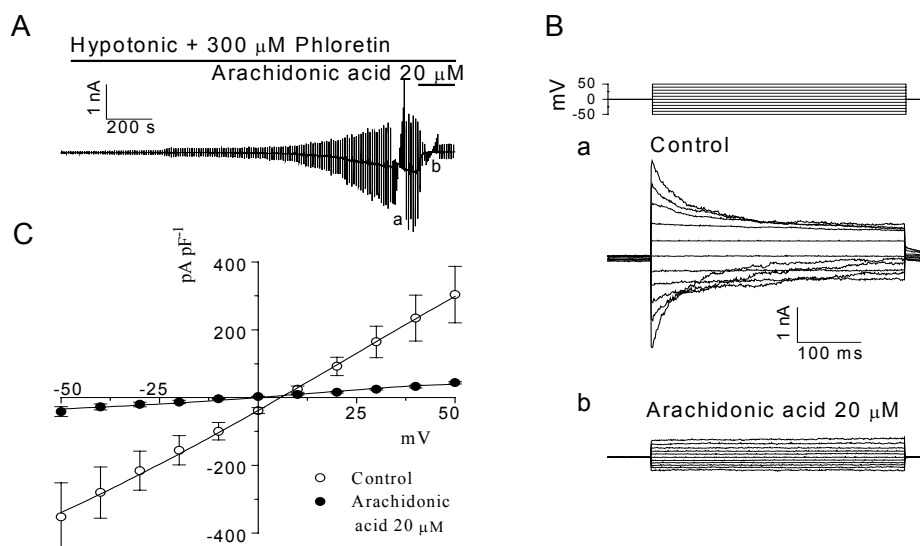


Figure 1. Swelling-activated, phloretin-insensitive chloride currents were inhibited by arachidonic acid in C127 cells.

(A) Representative record during application of alternating pulses from 0 to ± 25 mV (every 10 s) or of step pulses from -50 to $+50$ in 10 mV increments before (a) and after (b) application of arachidonic acid. Horizontal bars indicate the time of application of hypotonic solution containing $300 \mu\text{M}$ phloretin in the absence and presence of arachidonic acid ($20 \mu\text{M}$). (B) Expanded traces of current responses to step pulses recorded at the time indicated by a and b in (A). The step-pulse protocol is shown in the top panel. (C) Current-voltage relationships measured at the beginning of the pulses in the absence (control: open circles) and presence of $20 \mu\text{M}$ arachidonic acid (filled circles). The whole-cell currents were normalized by the cell capacitance ($n=4$). The remaining current in the presence of arachidonic acid had a linear I-V relationship and a reversal potential of around 3 mV, suggesting a non-selective leak current.

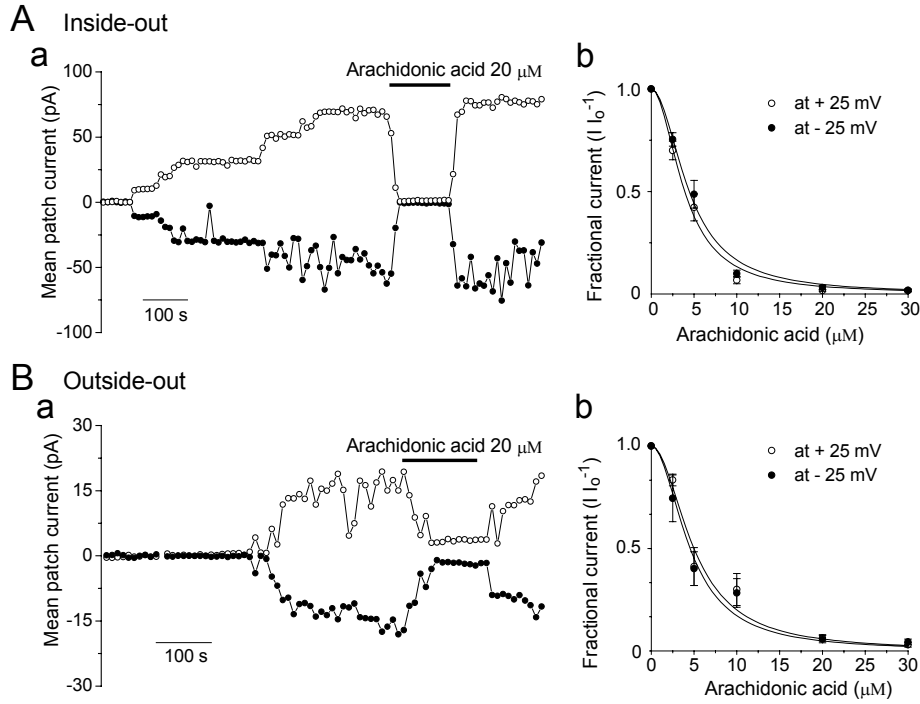


Figure 2. Macro-patch currents activated in inside-out (A) and outside-out patches (B) were reversibly suppressed by arachidonic acid in a dose-dependent manner.

(a) Representative mean macropatch currents during application of alternating pulses from 0 to ± 25 mV (every 10 s) are presented. Horizontal bars indicate the time of application of arachidonic acid (20 μ M). (b) Concentration dependence of arachidonate effects on VDACL currents recorded at ± 25 mV. All currents measured in the presence of arachidonate are normalized to the respective currents measured before arachidonate application (I_0). The inside-out data are fitted to Eqn. 1 with $K_d = 3.9 \pm 0.21$ μ M and 4.44 ± 0.23 μ M for outward and inward currents, respectively ($n=5 - 11$). The outside-out data are fitted to Eqn. 1 with $K_d = 4.99 \pm 0.44$ μ M and 4.54 ± 0.37 μ M for outward and inward currents, respectively ($n=5 - 7$). The Hill coefficient was 2.

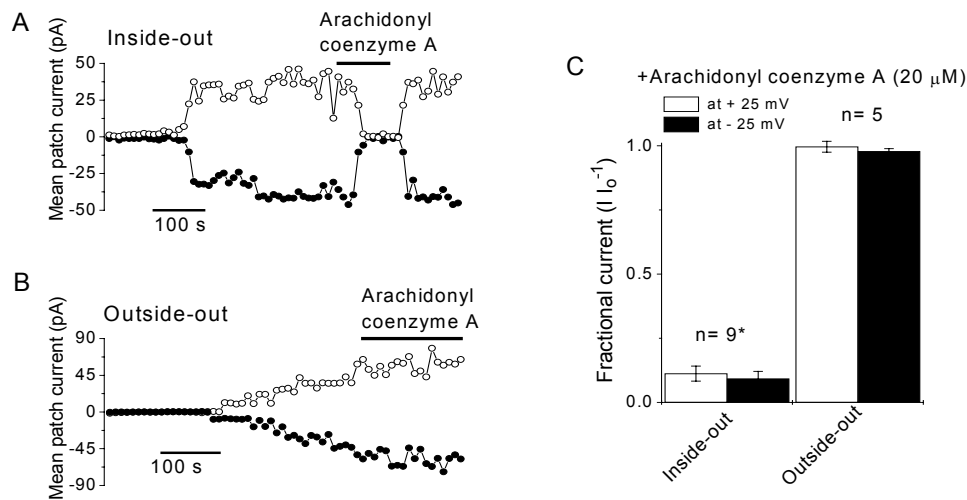


Figure 3. Effects of a membrane-impermeable analog of arachidonic acid, arachidonyl coenzyme A (20 μ M), on VDACL currents recorded at ± 25 mV from inside-out (A) and outside-out patches (B).

Representative mean macropatch currents during application of alternating pulses from 0 to ± 25 mV (every 10 s) are presented. Horizontal bars indicate the time of application of arachidonyl coenzyme A (20 μ M). (C) Macropatch currents in inside-out and outside-out patches in the presence of arachidonyl coenzyme A (20 μ M), normalized to those measured before application of arachidonyl coenzyme A (I_o).

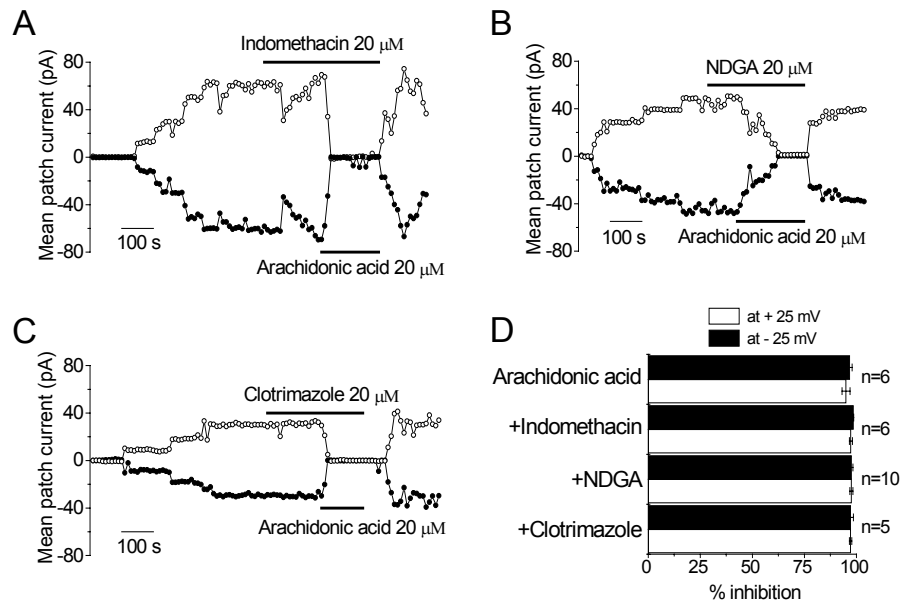


Figure 4. Suppression of macropatch currents in the inside-out mode by arachidonic acid was not affected by inhibitors of oxygenases that are involved in arachidonic acid metabolism.

(A) Effect of arachidonic acid in the presence of 20 μ M indomethacin. (B) Effect of arachidonic acid in the presence of 20 μ M NDGA. (C) Effect of arachidonic acid in the presence of 20 μ M clotrimazole. (D) Inhibitory effect of arachidonic acid in the absence or presence of oxygenase inhibitors. Percent inhibition of macropatch currents by arachidonic acid in the presence or absence of oxygenase inhibitors was calculated from those measured before application of arachidonic acid.

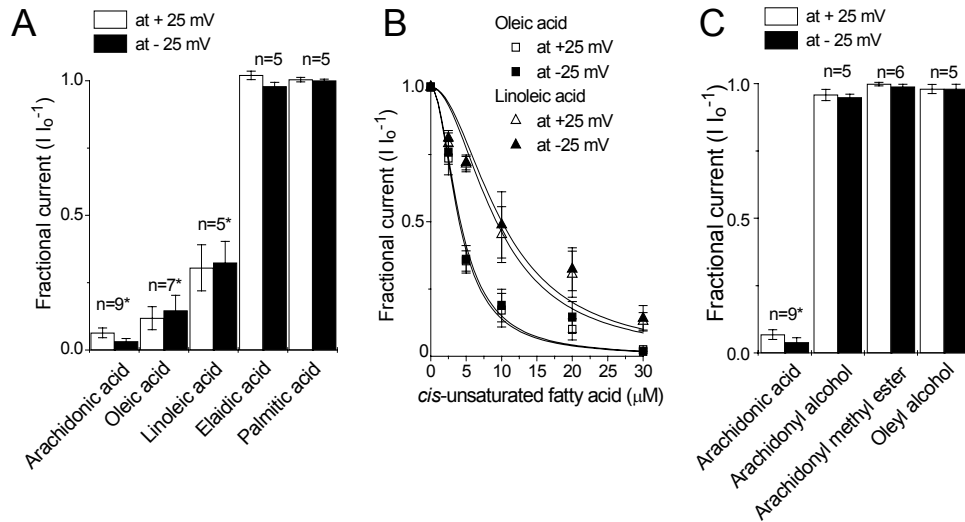


Figure 5. Role of the hydrophobic tail and polar head in inhibition of VDACL currents by arachidonic acid.

(A) Relative effects of *cis*-unsaturated (arachidonic, oleic and linoleic), *trans*-unsaturated (elaidic) and saturated (palmitic) fatty acids (all 20 μM) on macropatch currents recorded in the inside-out mode at ±25 mV. * Significantly different from control at $P < 0.001$. (B) Concentration-dependent inhibition of macropatch currents by oleic acid (squares) and linoleic acid (triangles). Open symbols are data for +25 mV and filled symbols are for -25 mV. The data are fitted to Eqn. 1 with $K_d = 4.02 \pm 0.21$ μM for +25 mV and $K_d = 4.19 \pm 0.34$ μM for -25 mV in the presence of oleic acid, and $K_d = 9.3 \pm 1.2$ μM for +25 mV and $K_d = 10.0 \pm 1.3$ μM for -25 mV in the presence of linoleic acid ($n = 5 - 7$). The Hill coefficient was 2. (C) Effects of non-charged arachidonic acid analogs, arachidonyl alcohol and methyl ester, and a non-charged oleate analog, oleyl alcohol, on VDACL macropatch currents in inside-out patches. Data are normalized to the mean current measured before application of drugs (I_0).

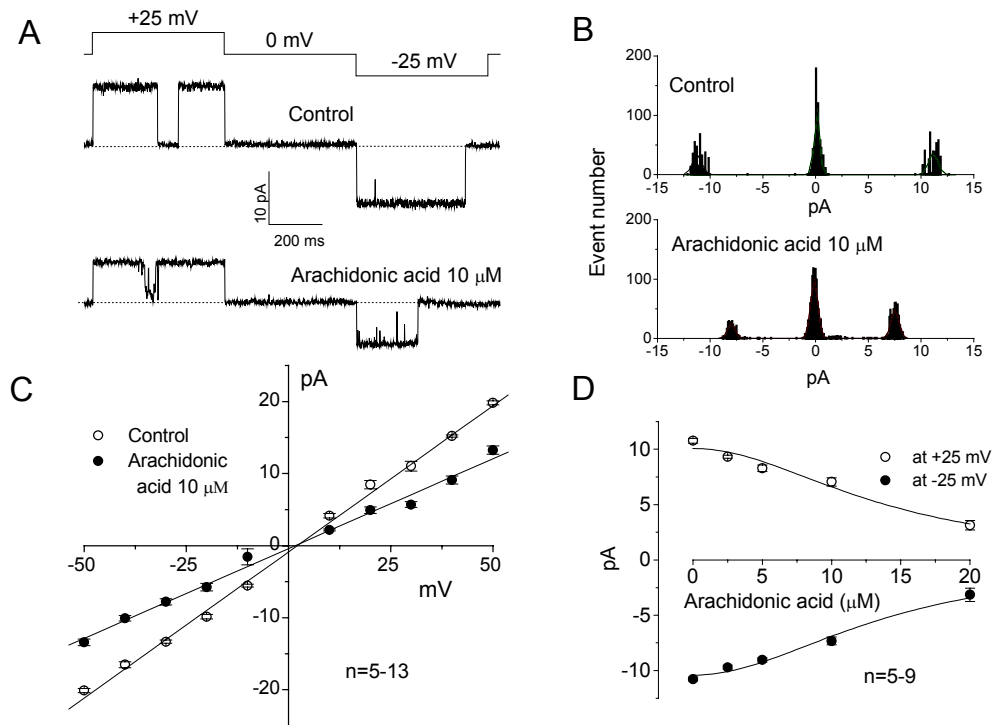


Figure 6. Effect of arachidonic acid added to the intracellular side on single VDACL channel currents recorded from inside-out patches.

(A) Representative current traces recorded during application of a step pulse from 0 to ± 25 mV in the absence (control) and presence of 10 μ M arachidonic acid. The pulse protocol is shown at the top of the traces. (B) Amplitude histograms of current traces presented in (A). (C) Unitary current-voltage relationships in the absence (control: open circles) and presence of 10 μ M arachidonic acid (filled circles). Mean single-channel conductance is 405.6 ± 6.4 pS for control and 249.2 ± 7.2 pS with 10 μ M arachidonic acid ($P < 0.05$, $n=5-13$). (D) Concentration-response curves of arachidonic acid effects on VDACL single-channel amplitude measured at ± 25 mV. The data are fitted to Eqn. 1 with $K_d = 13.8 \pm 1.6$ μ M and 14.0 ± 1.1 μ M for outward and inward currents, respectively ($n=5-9$). The Hill coefficient was 2.

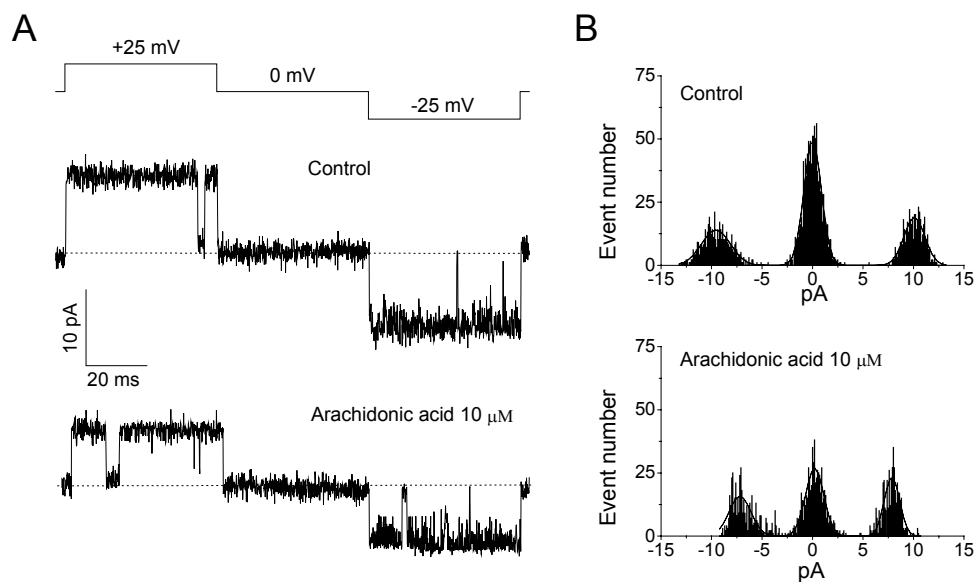


Figure 7. Fast reducing effect of arachidonic acid on single-channel current amplitude.

(A) Representative current traces recorded from an inside-out patch during application of a test pulse from 0 to ± 25 mV (protocol is shown at the top of the traces) by sampling at 10 kHz and filtering at 5 kHz in the absence (control: upper record) and presence of 10 μ M arachidonic acid (lower record). (B) Amplitude histograms for data presented in (A).

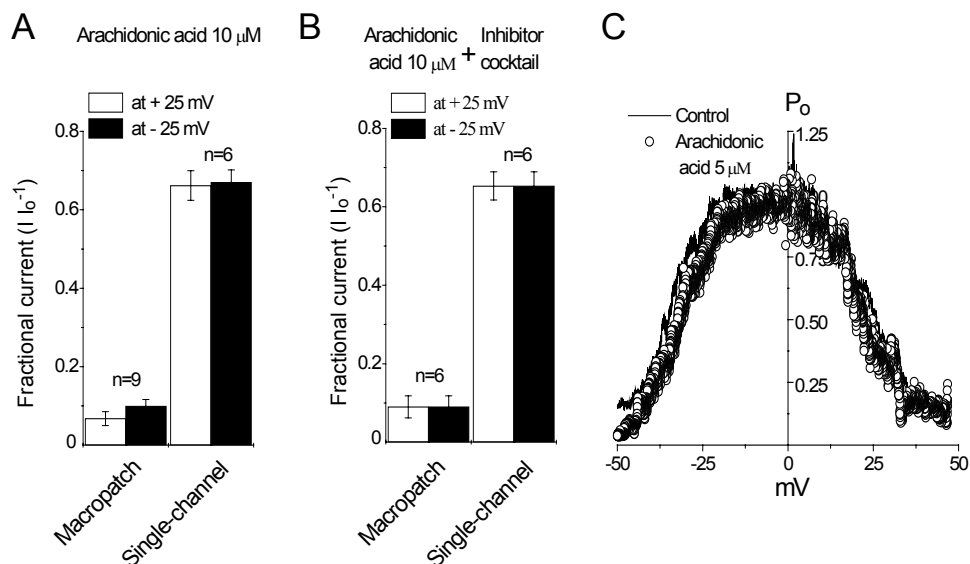


Figure 8. Effect of arachidonic acid on mean macropatch currents, single-channel amplitude and open-channel probability.

(A, B) Fractional macropatch and single-channel currents in inside-out patches in the presence of 10 μ M arachidonic acid without (A) and with (B) a cocktail of 3 oxygenase inhibitors (indomethacin, NDGA and clotrimazole, each 20 μ M). Data were normalized to the mean current measured before application of arachidonic acid (I_0). (C) Voltage dependence of steady-state open-channel probability. The data represent the ensemble-averaged current of 11 consecutive current responses to ramp pulses (from -50 mV to $+50$ mV at 10 mV/s rate) in the absence (control: solid line) and presence of 5 μ M arachidonic acid (open circles). The patch contained 5 – 6 channels. The P_o values were calculated as $P_o = (I/V)/G_{max}$, where I is the patch current, V is voltage and G_{max} is the maximal patch conductance at 0 mV.

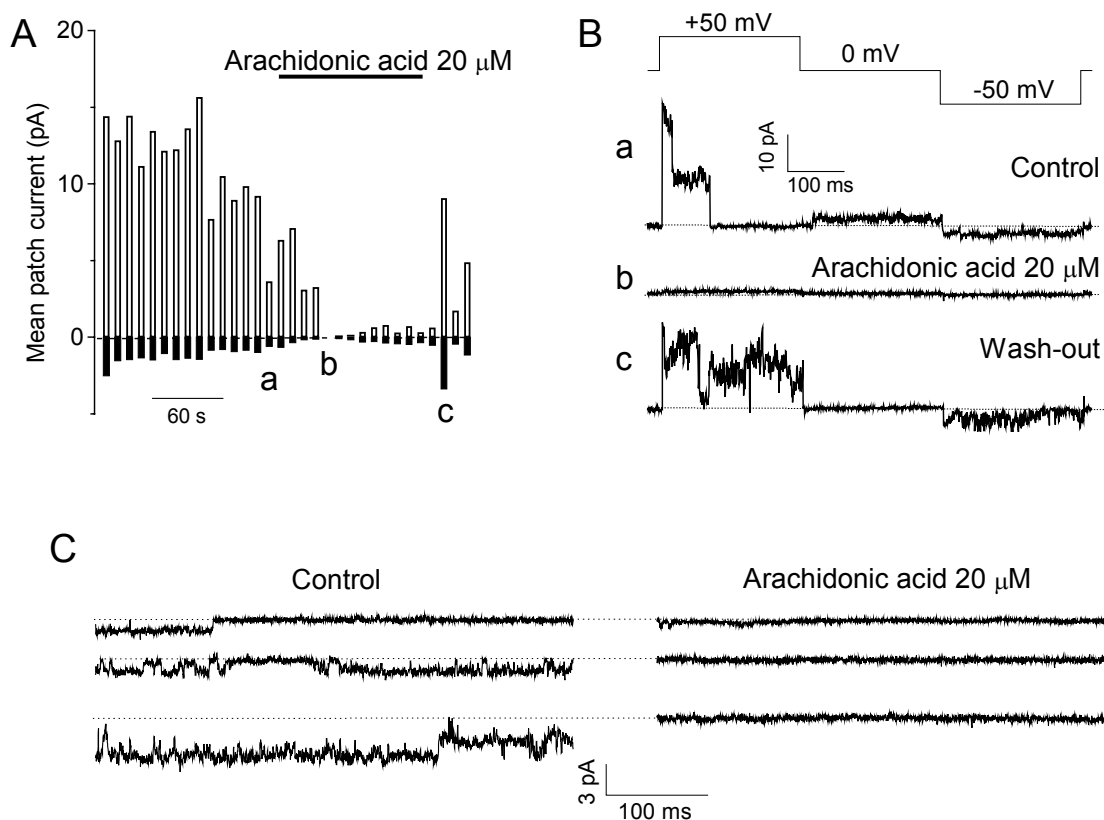


Figure 9. Arachidonic acid sensitivity of ATP current through VDACL channels.

(A) Mean patch currents in an inside-out patch measured at ± 50 mV. All anions in the bath were replaced with 100 mM ATP. Upper horizontal bar represents the time of arachidonic acid (20 μ M) application. Data represent 12 similar experiments. (a), (b) and (c) indicate the times when the traces in (B) were recorded. (B) Current traces recorded during application of alternating pulses from 0 to ± 50 mV (protocol is shown at the top of the traces) before application of arachidonic acid (a), in the presence of 20 μ M arachidonic acid (b), and after wash-out (c). (C) Representative inward ATP⁴⁻ currents recorded at -50 mV from three different patches before (left: control) and during (right) application of 20 μ M arachidonic acid.

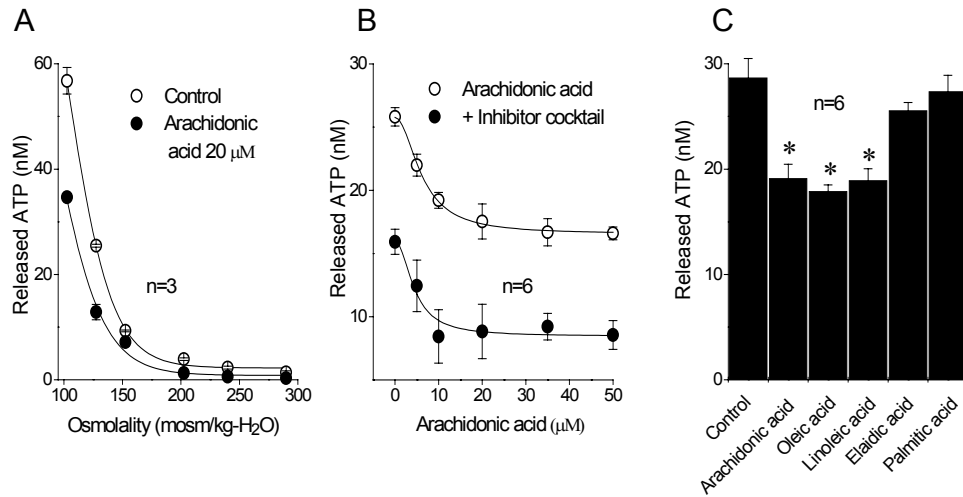


Figure 10. Effects of arachidonic acid and other fatty acids on swelling-induced ATP release from C127 cells.

(A) Swelling-induced ATP release as a function of medium tonicity in the absence (control: open symbols) and presence of 20 μ M arachidonic acid (filled symbols). (B) ATP release at 127.5 mosmol kg⁻¹ H₂O as a function of arachidonic acid concentration in the absence (control: open circles) and presence of inhibitors of arachidonic acid metabolism (indomethacin, NDGA, clotrimazole, 20 μ M each: filled circles). The data are fitted to Eqn. 2 with $K_d = 6.2 \pm 0.3$ μ M for control and $K_d = 4.4 \pm 1.2$ μ M for ATP release in the presence of metabolic inhibitors ($n=6$). The Hill coefficient was 2. (C) Relative effects of *cis*-unsaturated (arachidonic, oleic and linoleic), *trans*-unsaturated (elaidic) and saturated (palmitic) fatty acids (all 20 μ M) on ATP release measured at 127.5 mosmol kg⁻¹ H₂O. $n=6$. * Significantly different from control at $P < 0.01$.

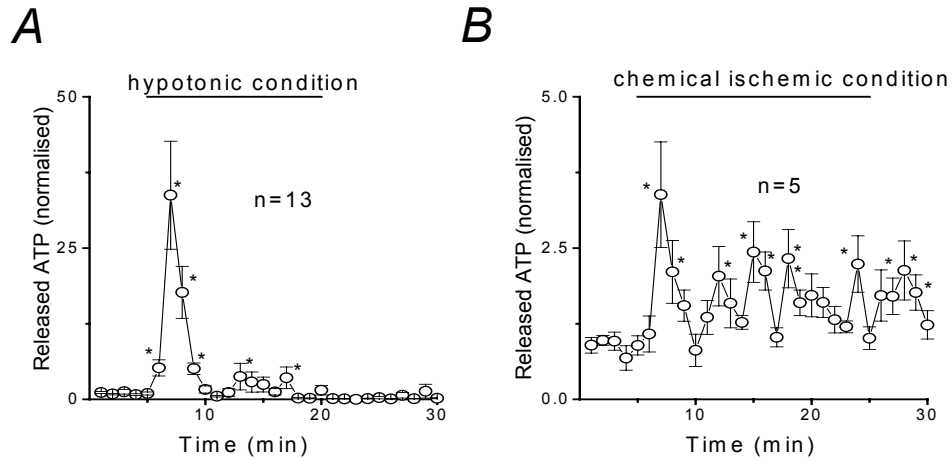


Fig.11. Hypotonic (A) and ischemic (B) condition induced ATP release from neonatal rat cardiomyocytes, detected by luciferin-luciferase ATP assay.
The solid bars represent period when control solution was replaced by either hypotonic or chemical ischemic solution (see Materials and Methods for details).

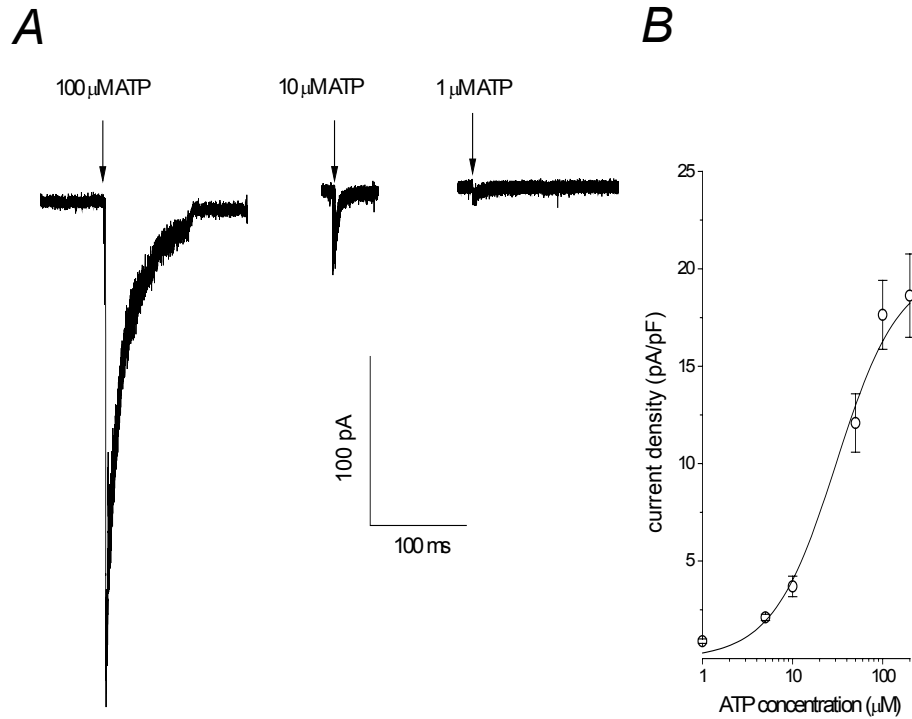


Fig.12. ATP-induced currents responses in PC12 cells, recorded at -50 mV upon puff application of ATP.

(A) Representative current traces before and after puff application of 100 μ M, 10 μ M and 1 μ M of ATP. (B) Concentration-response curve of the ATP-induced currents. Each symbol represents the mean peak current density of 3-7 observations (SE: *vertical bar*) in response to application of a single puff of ATP. The curve represents the best fit to the Hill equation with the half-maximal concentration (EC_{50}) of 30.4 ± 2.9 μ M and a Hill coefficient of 1.24, ($n=3-7$).

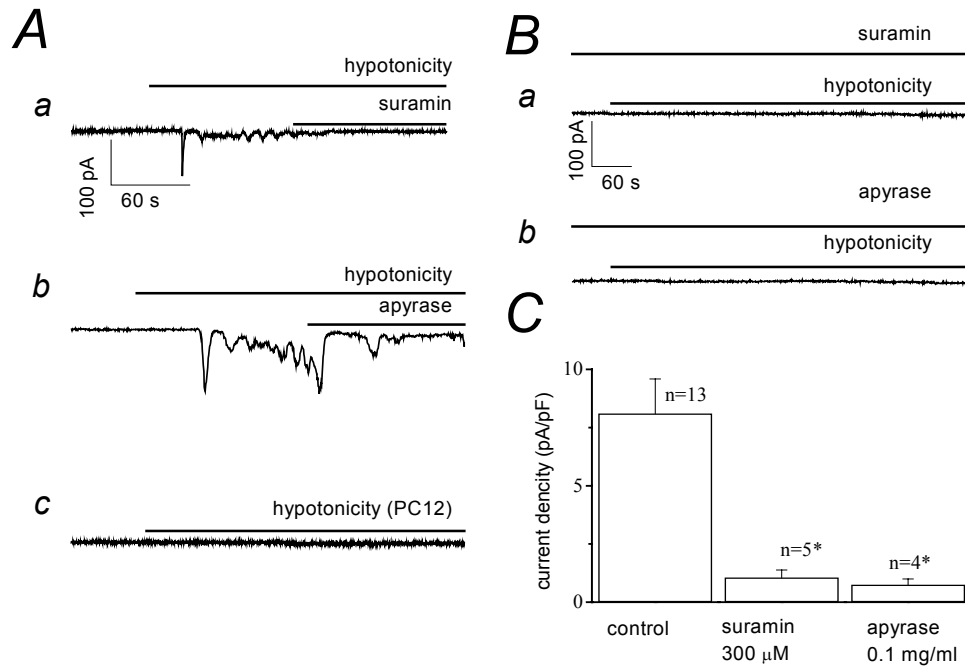


Fig.13. Hypotonicity induced current responses in PC12 cells, attached to single neonatal rat cardiomyocytes recorded at -50 mV.

(A) Representative current traces of ATP-spikes in hypotonic condition; these currents were inhibited upon application of suramin ($300\mu\text{M}$), (a) and apyrase (0.1 mg/ml), (b). (c) current trace when only PC12 cell was subjected to hypotonic condition. (B) PC12 current responses when cardiomyocytes were pretreated with of P_2 receptor blocker suramin $300\text{ }\mu\text{M}$ (a), and an ATP scavenger apyrase (0.1mg/ml) (b). (C) In this diagram, maximal current responses of PC12 cells are averaged before and after application of suramin and apyrase in experiments similar to those shown in (A). * Significantly different from control at $P < 0.05$.

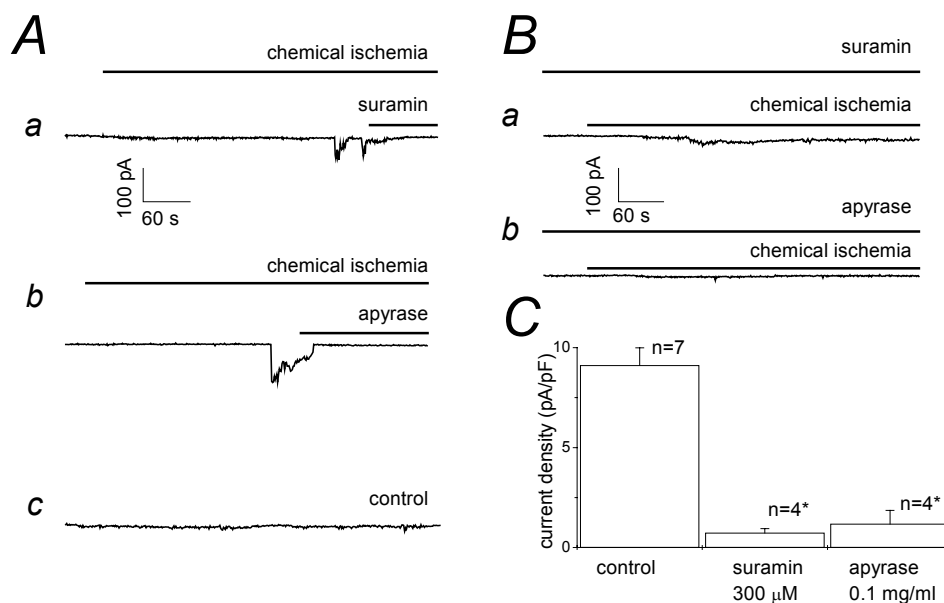


Fig.14. Chemical ischemia induced current responses in PC12 cells, attached to single neonatal rat cardiomyocytes recorded at -50 mV.

(A) Representative current traces of ATP-spikes in ischemic condition; these currents were inhibited upon application of suramin ($300\mu\text{M}$), (a) and apyrase (0.1 mg/ml), (b). (c) current recording from a PC12 cell attached to a single cardiac myocyte in control condition. (B) PC12 current responses when cardiomyocytes were pretreated with of P_2 receptor blocker suramin $300\text{ }\mu\text{M}$ (a), and an ATP scavenger apyrase (0.1mg/ml) (b). (C) In this diagram, maximal current responses of PC12 cells are averaged before and after application of suramin and apyrase in experiments similar to those shown in (A). * Significantly different from control at $P < 0.05$.

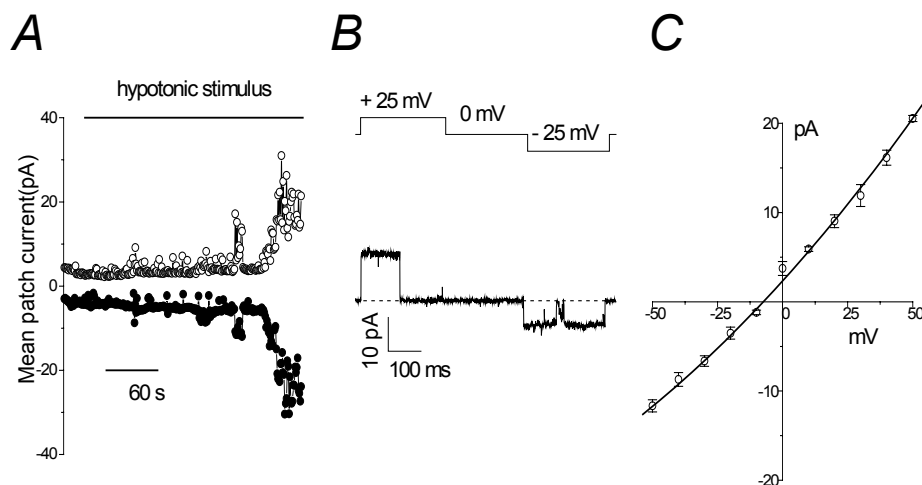


Fig.15 Hypotonicity induced activation of single-channel currents of large amplitude in on-cell patches.

(A) Representative patch currents during application of alternating pulses from 0 to ± 25 mV (every 10 s) in an on-cell patch. (B) Representative current traces recorded under hypotonic condition from on-cell patch, (voltage protocol is shown at the top of the traces). (C) Unitary I-V relationships recorded in cell-attached patches on neonatal rat cardiomyocytes (open circles).

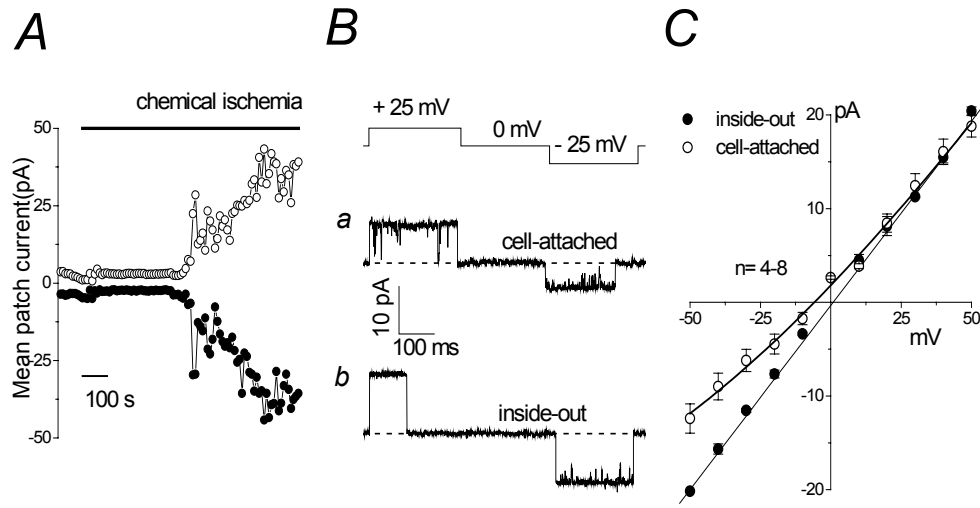


Fig.16. Ischemic condition induced activation of single-channel currents of large amplitude in on-cell patches.

(A) Representative patch currents during application of alternating pulses from 0 to ± 25 mV (every 10 s) in an on-cell patch. (B) Representative current traces recorded under ischemic condition from on-cell patch (a) and in control condition from inside-out patch (b); (protocol is shown at the top of the traces). (C) Unitary i-V relationships recorded from cell-attached patches on neonatal rat cardiomyocytes (open circles) and from inside-out patches (closed circles).

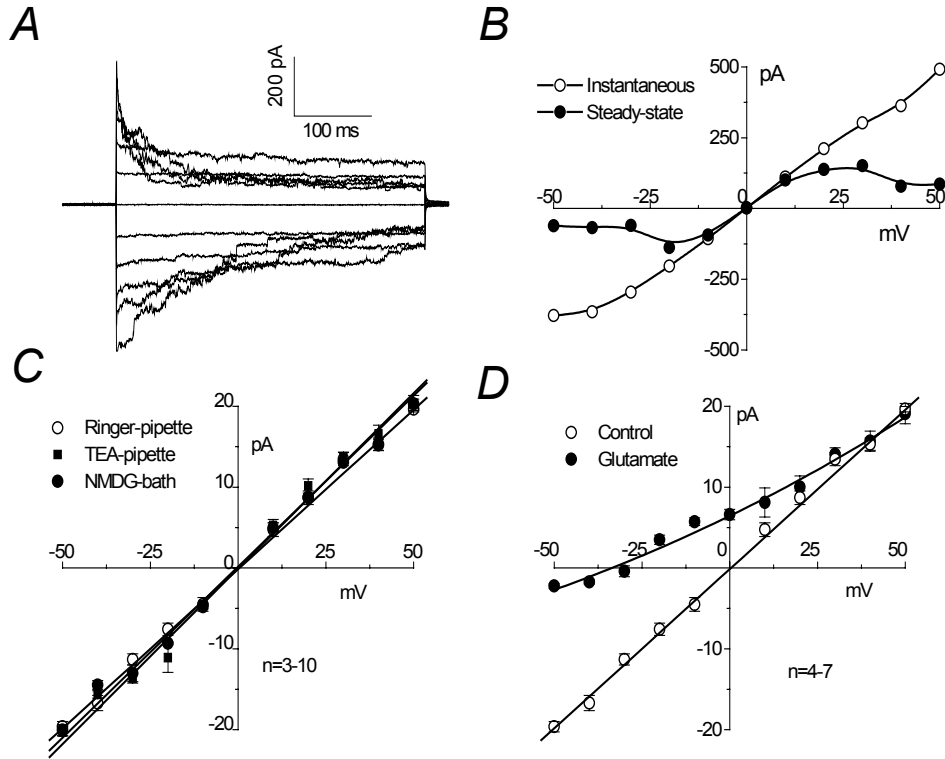


Fig.17. Voltage-dependent inactivation and anion selectivity of single large conductance channel currents.

(A) Representative current traces recorded upon application of step pulses from 0 to ± 50 mV in 10 mV increments in a macro-patch excised from a neonatal rat cardiomyocytes. (B) I-V relationship of instantaneous (open circles) and steady-state (closed circles) currents, from the recording shown in A, measured at the beginning and end of the current responses to step pulses. (C) Single-channel i-V relationship of large conductance channels in control conditions (normal Ringer solution in the bath and pipette, open circles), after substitution of monovalent cations with NMDG in the bath (closed circles) or with TEA in the pipette solution (closed squares); (D) Effect of replacement of bath Cl^- with glutamate (closed circles); i-V in symmetrical Ringer solution is plotted as open circles. $P_{\text{Cl}}/P_{\text{glutamate}} = 0.21 \pm 0.02$.

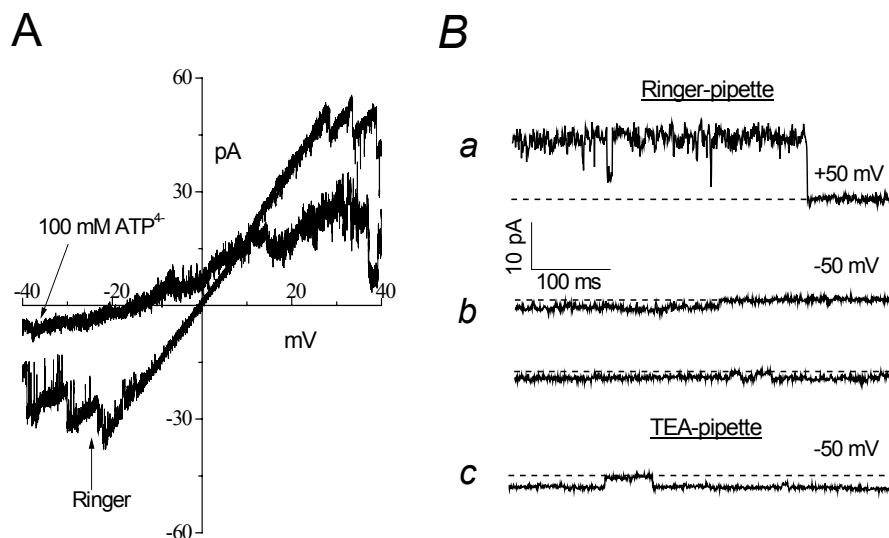


Fig.18. ATP permeability of large conductance anion channel recorded from inside-out patches excised from neonatal rat cardiomyocytes.

(A) Representative ramp I-V records from a macro-patch in normal Ringer solution in the bath and after the bath solution was replaced 100 mM ATP. Pipette solution was normal Ringer. (B) Representative single-channel currents recorded at +50 mV (a) and -50 mV (b) and (c) in the presence of 100 mM ATP in the bath. The pipette solution was normal Ringer for (a) and (b) and TEA for (c). Single-channel amplitude for outward Cl^- current at +50 mV was 12.32 ± 0.32 pA ($n=8$) and for inward ATP^{4-} current at -50 mV was -1.88 ± 0.11 pA ($n=8$, Ringer pipette), and -1.84 ± 0.12 pA ($n=10$, TEA pipette).

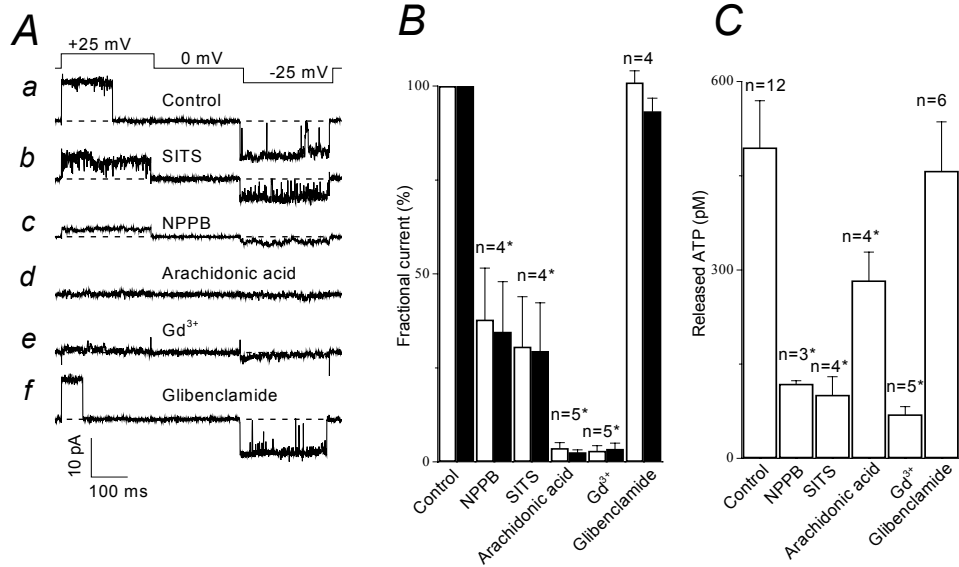


Fig.19. Pharmacological profile of large conductance anion channel and hypotonicity induced ATP release from neonatal rat cardiomyocytes.

(A) Representative current traces recorded from excised inside-out and outside-out (only for Gd^{3+}) patches, in control (a), and in the presence of SITS (100 μ M), NPPB (100 μ M), arachidonic acid (20 μ M), Gd^{3+} (50 μ M), and glibenclamide (200 μ M) (b,c,d,e, and f, respectively). (B) Effects of drugs on mean macro-patch currents recorded at +25 mV (open bars) and -25 mV (closed bars). Data were normalized to the mean current measured before application of drugs after correction for the background current. Each column represents the mean \pm SEM. * $P < 0.02$ vs. control. (C) Effects of drugs on hypotonicity induced ATP release from neonatal rat cardiomyocytes. Here, the maximal level of ATP concentration in the hypotonic superfusate is corrected for the background ATP level before hypotonic challenge. * Significantly different from the control at $P < 0.05$.

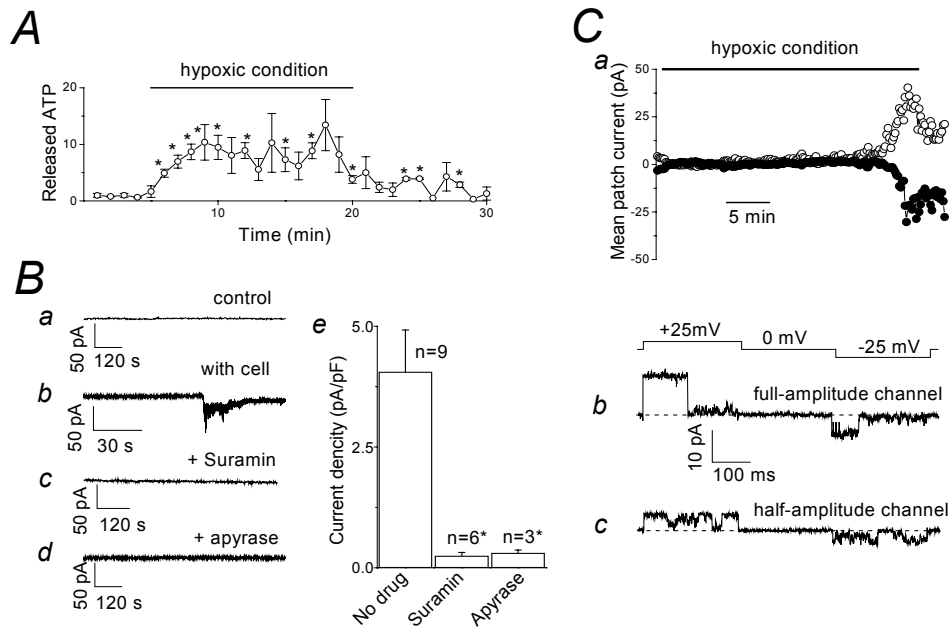


Fig.20. ATP release and channel activity in hypoxic conditions.

(A) Time-dependent ATP release from primary culture of neonatal rat cardiomyocytes, induced by hypoxic condition (100% argon gas bubbling), detected by luciferin/luciferase ATP assay method (n=3). (B) ATP release from cardiomyocytes in hypoxic condition detected by biosensor technique. Representative current records from voltage-clamped (at -50 mV) PC12 cells placed on the top of cardiac myocytes in ischemic conditions (applied from $t=0$ time) without (a) and with cardiac myocyte in close proximity (b). No ATP-spikes were detected when cells were pretreated with suramin ($300\mu\text{M}$) (c) and apyrase (0.1 mg/ml) (d) respectively. (e) Summarized data of hypoxia induced maximal current responses in the absence and presence of suramin ($300\mu\text{M}$) and apyrase (0.1 mg/ml). (C) Hypoxic condition activated large conductance channel in neonatal rat cardiomyocytes. (a) Representative patch currents during application of alternating pulses from 0 to ± 25 mV (every 10 s) in an on-cell patch. (b) and (c) Representative current trace of full-amplitude (b) and half-amplitude maxi-channels recorded under hypoxic condition in cell-attached patch (voltage protocol is shown on the top of the traces).

* Significantly different from control at $P < 0.05$.

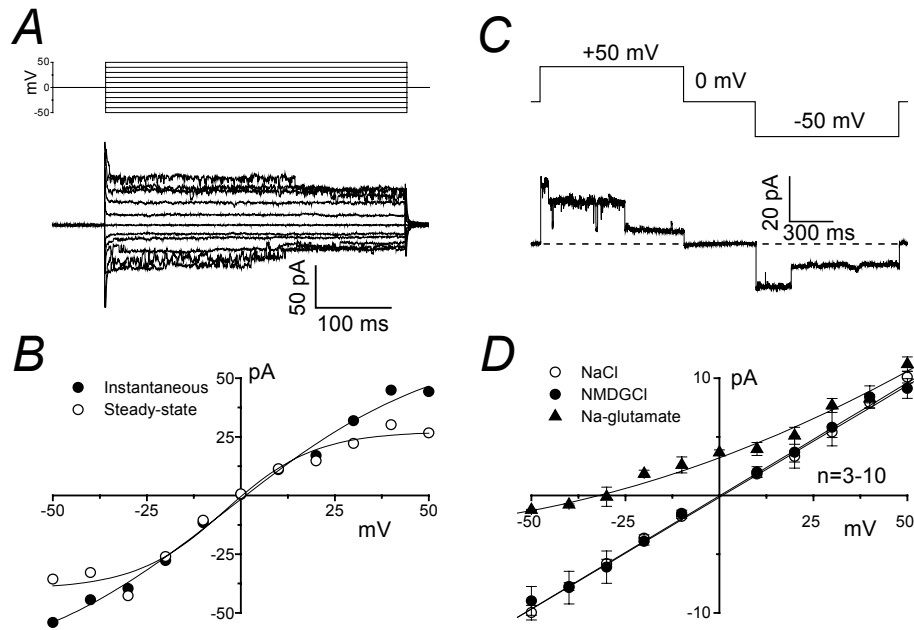


Fig.21. Biphysical profile of half-amplitude channels activated upon hypoxia in cardiomyocytes.

(A) Representative current traces recorded upon application of step pulses from 0 to ± 50 mV in 10 mV increments in a macro-patch excised from a neonatal rat cardiomyocytes subjected to hypoxia. (B) I-V relationship of instantaneous (closed circles) and steady-state (open circles) currents, from the recording shown in A, measured at the beginning and end of the current responses to the step pulses. (C) Representative single-channel current trace recorded from inside-out patch (voltage protocol is shown on the top of the trace). (D) Effect of replacement of bath Na^+ with NMDG $^+$ (closed circles) and Cl^- with glutamate (closed triangles); i-V in symmetrical Ringer solution is plotted as open circles. $P_{\text{Cl}}/P_{\text{glutamate}} = 0.22 \pm 0.03$.

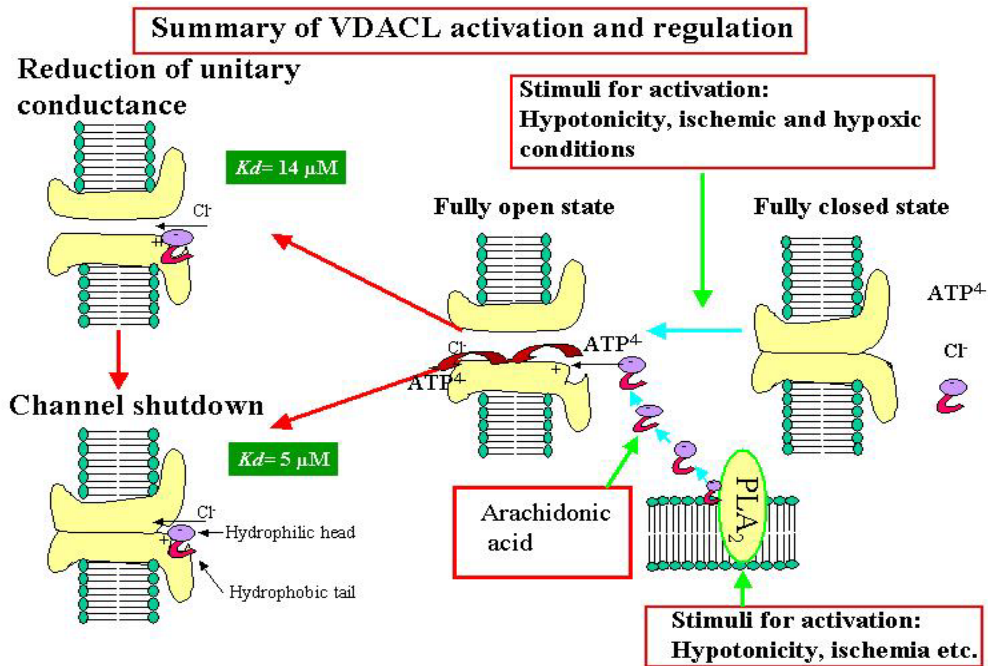


Fig.22. Schematic model of VDACL activation and regulation.

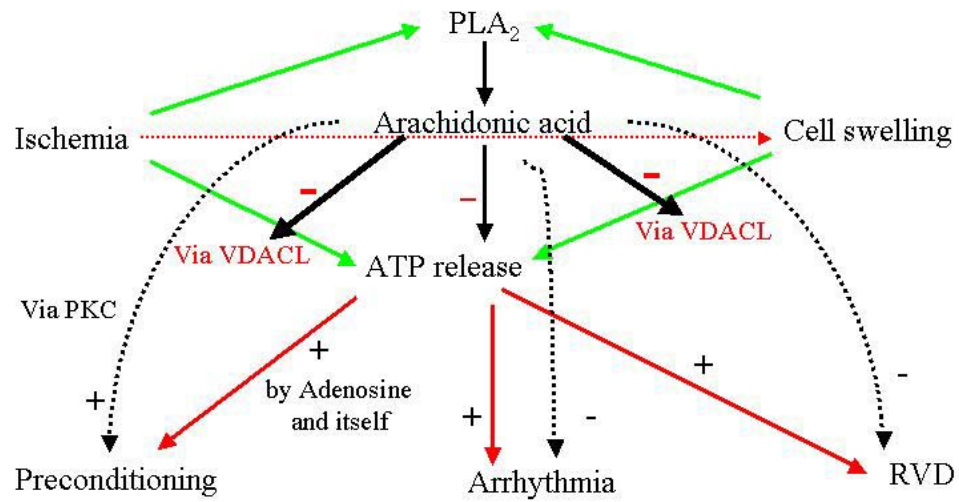


Fig.23. Relation between ATP and arachidonic acid release upon various stimuli, and their importance in pathophysiological conditions, like cell swelling and ischemia.